

Accepted Manuscript

Novel indole and triazole based hybrid molecules exhibit potent anti-adipogenic and antidyslipidemic activity by activating Wnt3a/ β -catenin pathway

Sujith Rajan, Surendra Puri, Durgesh Kumar, Madala Hari Babu, Kripa Shankar, Salil Varshney, Ankita Srivastava, Abhishek Gupta, M. Sridhar Reddy, Anil N. Gaikwad



PII: S0223-5234(17)30826-7

DOI: [10.1016/j.ejmech.2017.10.034](https://doi.org/10.1016/j.ejmech.2017.10.034)

Reference: EJMECH 9826

To appear in: *European Journal of Medicinal Chemistry*

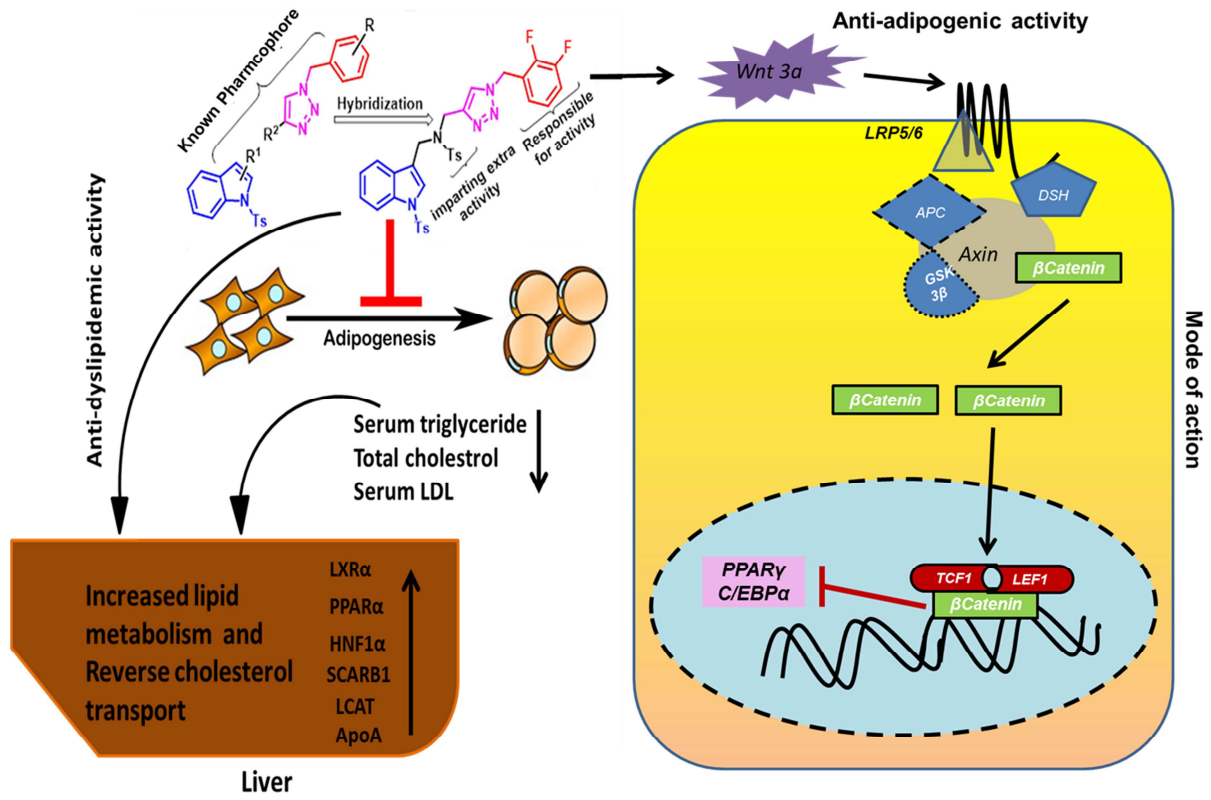
Received Date: 11 July 2017

Revised Date: 5 October 2017

Accepted Date: 11 October 2017

Please cite this article as: S. Rajan, S. Puri, D. Kumar, M.H. Babu, K. Shankar, S. Varshney, A. Srivastava, A. Gupta, M.S. Reddy, A.N. Gaikwad, Novel indole and triazole based hybrid molecules exhibit potent anti-adipogenic and antidyslipidemic activity by activating Wnt3a/ β -catenin pathway, *European Journal of Medicinal Chemistry* (2017), doi: 10.1016/j.ejmech.2017.10.034.

This is a PDF file of an unedited manuscript that has been accepted for publication. As a service to our customers we are providing this early version of the manuscript. The manuscript will undergo copyediting, typesetting, and review of the resulting proof before it is published in its final form. Please note that during the production process errors may be discovered which could affect the content, and all legal disclaimers that apply to the journal pertain.



**Novel Indole And Triazole Based Hybrid Molecules Exhibit Potent Anti-Adipogenic
And Antidyslipidemic Activity By Activating Wnt3a/ β -Catenin Pathway**

**Sujith Rajan^{1,2}, Surendra Puri³, Durgesh Kumar^{1,2}, Madala Hari Babu³, Kripa Shankar¹,
Salil Varshney^{1,2}, Ankita Srivastava^{1,2}, Abhishek Gupta¹, M Sridhar Reddy^{3*}, Anil N
Gaikwad^{1,2#}.**

¹Division of Pharmacology, CSIR-Central Drug Research Institute, Lucknow - 226031, India

²Academy of Scientific and Innovative Research, CSIR-CDRI.

³Division of Medicinal and Process Chemistry, CSIR-Central Drug Research Institute, Lucknow
- 226031, India.

#Corresponding Authors: Anil Nilkanth Gaikwad, Division of Pharmacology, CSIR-Central
Drug Research Institute, Lucknow, Uttar Pradesh, India.

Tel.: +91 522 2771940x4876; **fax:** +91 522 2771941

E-mail: anil_gaikwad@cdri.res.in

M Sridhar Reddy, Division of Medicinal and Process Chemistry, CSIR-Central Drug Research
Institute, Lucknow - 226031, India.

E-mail: msreddy@cdri.res.in

Abstract

Obesity and dyslipidemia is the two facet of metabolic syndrome, which needs further attention. Recent studies indicate triazole and indole derivatives have remarkable anti-obesity/antidyslipidemic activity. To harness the above-mentioned potential, a series of novel triazole clubbed indole derivatives were prepared using click chemistry and evaluated for anti-adipogenic activity. Based on the structure-activity relationship, essential functional groups which potentiate anti-adipogenic activity were identified. The lead compound **13m** exhibited potent anti-adipogenic activity compared to its parent compounds with the IC-50 value of 1.67 μ M. Further evaluation of anti-adipogenic activity was conducted in different cell lines such as C3H10T1/2 and hMSC with positive result. The anti-adipogenic effect of compound **13m** was most prominent in the early phase of adipogenesis, which is driven by the G1 to S phase cell cycle arrest during mitotic clonal expansion. The mechanistic study suggests that compound **13m** exhibit anti-adipogenic property by activating wnt3a/ β catenin pathway, a known suppressor of key adipogenic genes PPAR γ and C/EBP α . It is noteworthy that the compound **13m** also reduced serum triglyceride, LDL and total cholesterol in Syrian golden Hamster Model of dyslipidemia. The anti-adipogenic activity of compound **13m** can also be correlated with decreased expression of PPAR γ and increased expression of β -catenin in epididymal white adipose tissue (eWAT) *in vivo*. The compound **13m** also increased the expression of genes involved in reverse cholesterol transport (RCT) such as PPAR α and LXR1 α indicating another mechanism by which compound **13m** ameliorates dyslipidemia in Syrian golden hamster model. Overall this study provides a unique perspective into the anti-adipogenic/antidyslipidemic property of triazole and indole hybrids molecules with further scope to increase the anti-adipogenic potency for therapeutic intervention of obesity and metabolic syndrome.

Introduction

Obesity is a major risk factor for insulin resistance, type 2 diabetes mellitus (T2DM), hypertension and cardiovascular diseases collectively known as metabolic syndrome [1]. There has been a startling increase in the rate of obesity worldwide. Even though 62% of obese individuals live in the developed nation, the percentage of obese people in developing countries are also increasing exponentially [2]. Obesity mainly results from excess energy intake than energy expenditure [3]. and the excess energy is stored in adipose tissue in the form of lipid droplets [4]. There are many factors contributing to obesity such as lack of physical activities, sedentary lifestyle etc. Excess storage of lipid in adipocytes leads to hypertrophy (increase in size) and hyperplasia (increase in number) [5]. The overall gain in adipose tissue mass is associated with T2DM, metabolic syndrome and cardiovascular diseases [6]. 10% adipocytes are renewed every year to maintain healthy adipose tissue by a process called adipogenesis [7]. Recent studies in adipocyte biology have given better understanding of molecular mechanism linking obesity to other disease conditions such as insulin resistance, type 2 diabetes [8]. As adipocytes play a major role in glucose homeostasis and insulin resistance, they have been targeted as the therapeutic intervention for treatment of insulin resistance and associated metabolic syndrome [9]. Inhibiting adipogenesis and thereby limiting overall increase in adipose tissue mass is seen as a potential mechanism for the treatment and prevention of obesity. Therefore, chemical agents exhibiting such inhibitory effect on adipogenesis are of great pharmacological importance.

The process of adipogenesis has been well studied in different murine cell lines such as 3T3-L1, 3T3-F442A and C3H10T1/2 [10]. Adipogenesis is complex process accompanied with a cascade of changes in morphology, protein expression, hormonal sensitivity and extracellular matrix. The

process of adipogenesis can be divided into four stages 1) Growth arrest, 2) Mitotic clonal expansion, 3) Early differentiation and 4) Late differentiation [11, 12]. After growth arrest cells upon hormonal stimulation undergo two to three rounds of cell division termed as mitotic clonal expansion, a process essential for adipogenesis. At the early stage of adipogenesis, genes involved in lipogenesis and fatty acid metabolism such as fatty acid synthase (FAS), adipocyte-specific fatty acid binding protein (AP2), and lipoprotein lipase (LPL) etc., get activated. At the late stage, adipocytes start secreting proteins such as leptin, adiponectin, resistin etc, which are collectively called as adipokines [13]. Each stage of adipogenesis is governed by different transcription factors such as CCAAT/enhancer binding protein α and β (C/EBP α and C/EBP β), peroxisome proliferator-activator receptor γ (PPAR γ) etc [14]. These transcription factors through a cascade of signaling, activates adipocyte-specific genes resulting in the formation of fully matured adipocytes. Gene mutation studies conducted on mouse 3T3-L1 show PPAR γ as the master regulator of adipogenesis [15]. PPAR γ agonists like thiazolidinedione class of compound are known for their pro-adipogenic activity [16].

Molecular hybridization approach is a straightforward and emerging approach for the rational design of new prototypes and structural modifications based on the recognition of pharmacophoric subunits [17]. Indole derivatives are endowed with diverse pharmacological properties including anti-tubercular [18], anticancer [19], antioxidant [20] and antiviral [21] activities. Owing to the broad spectrum of pharmacological profile, eliciting anti-obesity [22] lipid lowering [23] and anti-adipogenic [24] activity of indole derivatives has been widely investigated. On the other hand, it is well documented that 1,4-disubstituted 1,2,3-triazoles display a number of chemotherapeutic properties such as anticancer [25], antifungal [26], anti-tubercular [27], antimicrobial [28], antiviral [29], anti-HIV [30], anti-inflammatory [31], anti-

HSV [32], anticonvulsant [33] along with significant anti-adipogenic activities [34]. The aforementioned findings led us to explore molecular hybridization approach and synthesize new functionalized indoles and 1,2,3-triazoles to generate a new prototype for biological evaluation. The structure activity relationship (SAR) study of functionalized hybrid analogues was done around the lead compound **13m**.

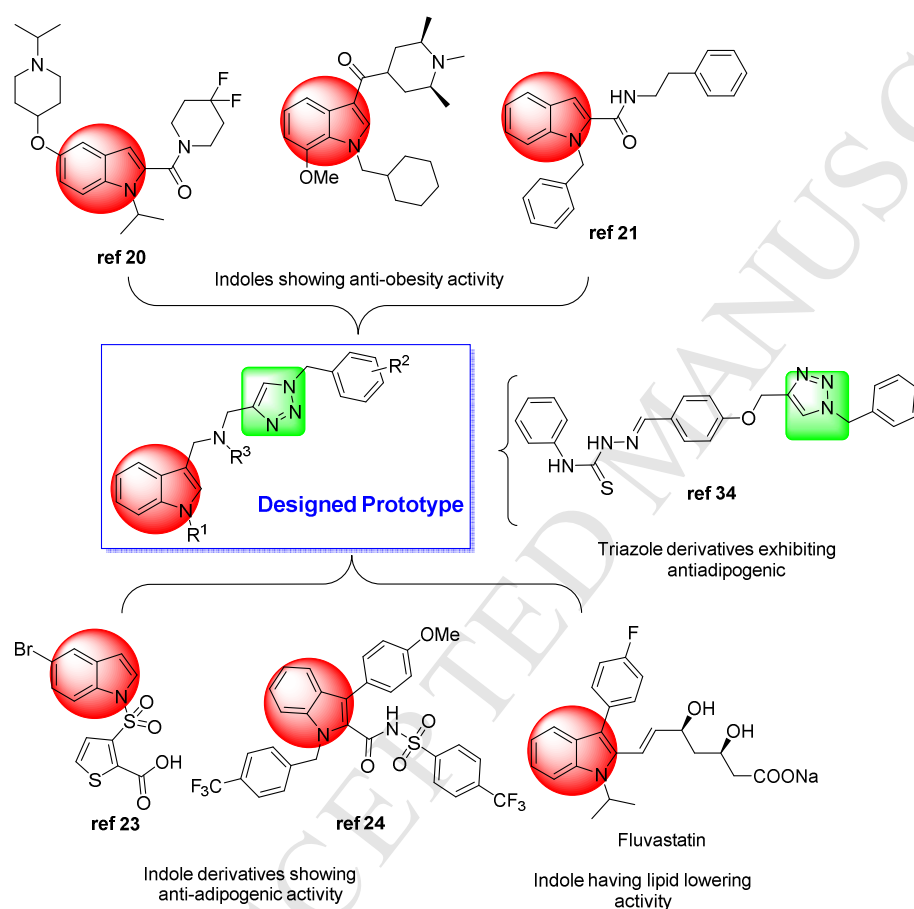


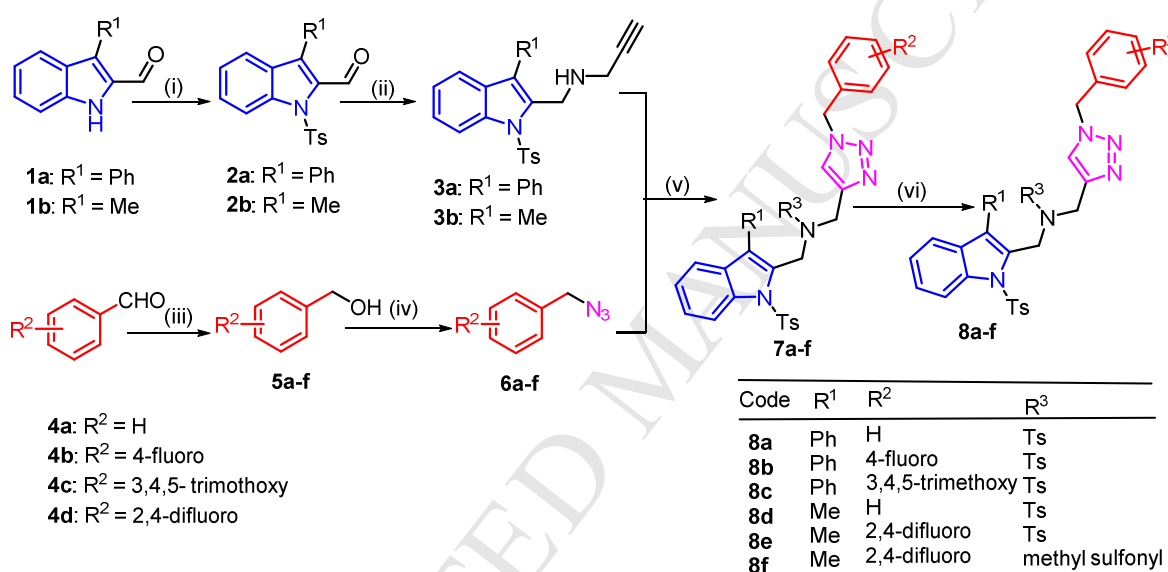
Figure 1. Schematic representation of indole and triazole hybrid prototypes based on reported antidi-lipidemic and anti-obesity candidates.

Results and Discussion

Chemistry: The synthesis of desired hybrid compounds was started from indole carboxaldehyde derivatives. The 3-substituted indole-2-carboxaldehyde derivatives **1a-b** were prepared by using

literature procedure [35] and was further treated with TsCl in the presence of DMAP, TEA in DCM to obtain the sulfonylated indole derivatives **2a-b**. Condensation of compounds **2a-b** with propargyl amine followed by reduction with NaBH₄ afforded the terminal alkyne derivatives **3a-b**.

Scheme 1. Synthetic Route To 2-Substituted Indole And Triazole Based Hybrid Molecules 8a-f.



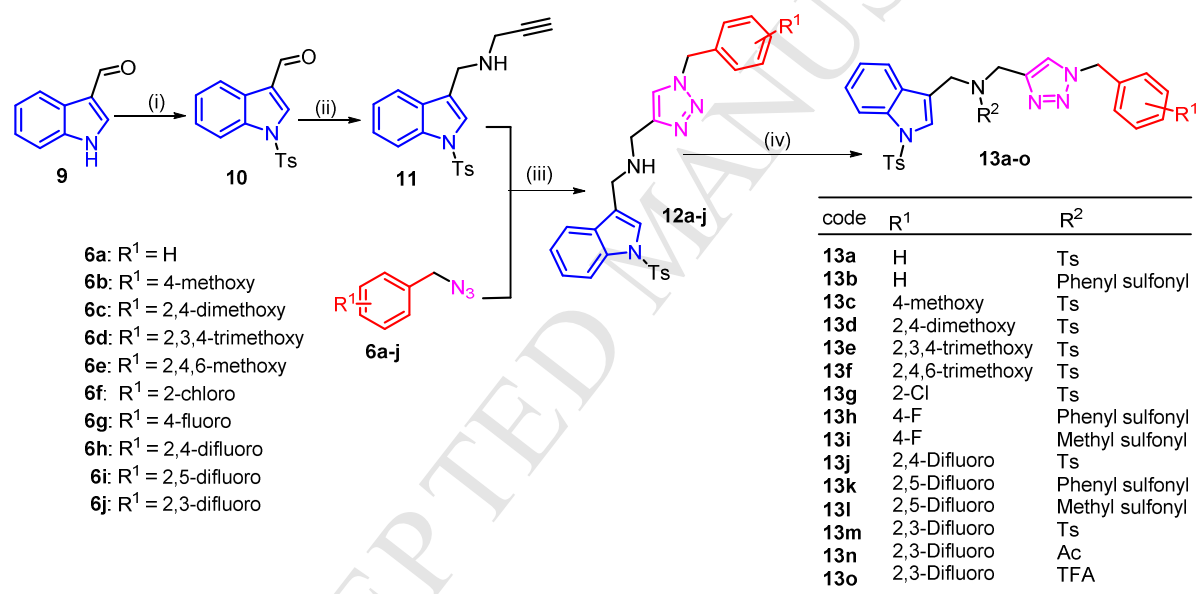
Reagents and conditions: (i) TsCl, DMAP, TEA, DCM, 0 °C to rt, 4 h; (ii) propargyl amine, DCE, NaBH₄, MeOH, 0 °C to rt 4 h; (iii) NaBH₄, MeOH, 0 °C to rt, 4 h; (iv) PPh₃, NaN₃, DMF:CCl₄ (4:1), 90 °C, 12 h; (v) DIPEA, CuI, THF:DMF (1:1), rt, 2-4 h; (vi) sulfonyl chloride, DMAP, TEA, DCM, rt, 4 h.

The azide derivatives **6a-d** for click reaction was prepared from readily available benzaldehyde derivatives **4a-d** via reduction followed by nucleophilic substitution reactions with sodium azide. It involves CuI catalyzed 3+2 cycloaddition reaction of benzylazides **6a-d** and terminal alkynes **3a-b** that produced the triazole clubbed indole derivatives **7a-f** in good yields. Finally, the sulfonyl protection of **7a-f** with desired sulfonyl chlorides produced the target compounds **8a-f** in good to excellent yields.

Scheme 2. Synthetic Route To 3-Substituted Indole And Triazole Based Hybrid Molecules

13a-o.

To further prepare a library of compounds, readily available indole-3-carboxamide was opted as a starting material. By using aforementioned synthetic strategy, the considerable number of N-sulfonyl 3-substituted indole and triazole based hybrid molecules **13a-m** were prepared. Based on the preliminary results obtained from *in vitro* screening the possible structural modifications were done around **13m**. In this series acetylation and trifluoro acetylation was carried out on **12f** to obtain **13n** and **13o** respectively.

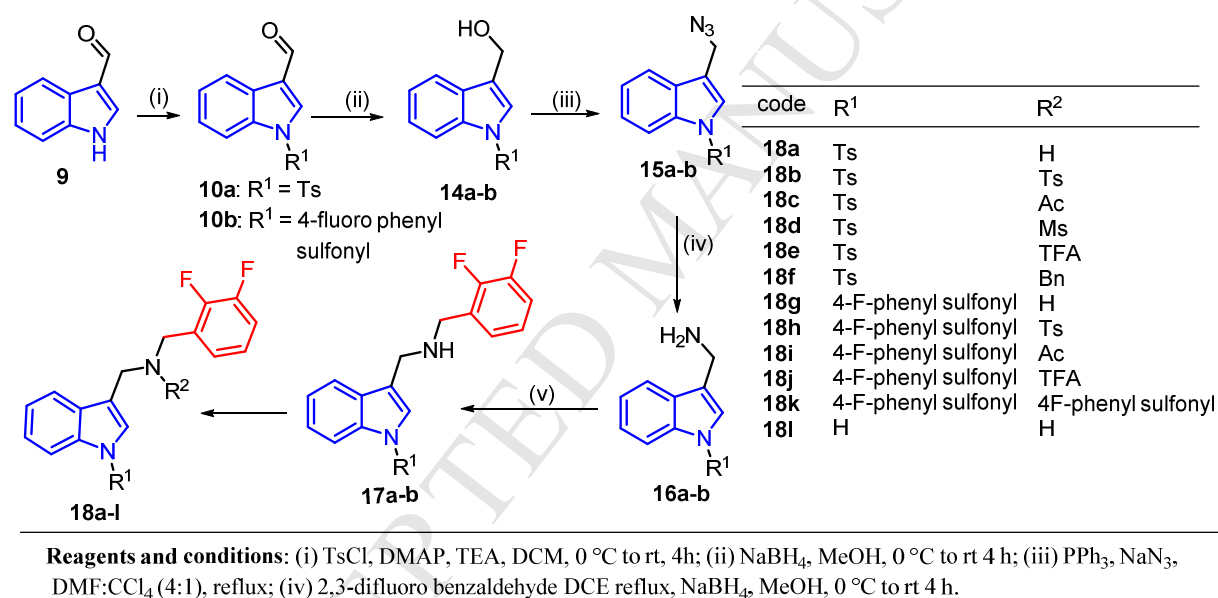


Reagents and conditions: B) (i) TsCl, DMAP, TEA, DCM, 0 °C to rt, 4 h; (ii) propargyl amine, DCE, NaBH₄, MeOH, 0 °C to rt 4 h; (iii) Cul, DIPEA, THF:DMF (1:1) rt, 2-4 h; (iv) Sulfonyl chloride (or) Acetyl chloride, DMAP, TEA, DCM, rt, 4 h.

Scheme 3. Synthetic Routes To 3-Substituted Indole And 2,3-Difluoro Benzaldehyde Based Hybrid Molecule 18a-l

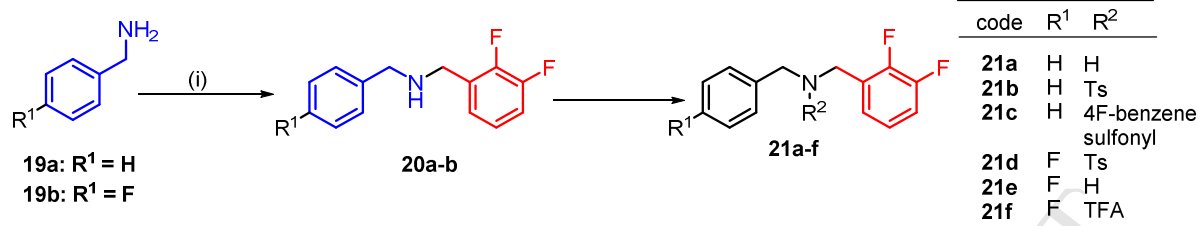
Further, the role of indole and triazole pharmacophores around the lead compound **13m** showing anti-adipogenic activity was tested. Initially, triazole ring was removed from the hybrid molecule **13m** to know the structure activity relationship (SAR) as well as the activity of newly synthesized compounds. The synthesis of the desired prototype started from the reduction of

sulfonyl protected indole-3-aldehyde derivatives **10a-b** followed by the reduction with NaBH_4 afforded compounds **14a-b**. Nucleophilic displacement of the hydroxyl group on **14a-b** was achieved by treating with sodium azide and triphenyl phosphine in DMF and CCl_4 (4:1 ratio respectively) as a solvent. Further, the reduction of azide group with PPh_3 in THF: H_2O (6:1 ratio respectively) produced **16a-b**. Condensation of **16a-b** with 2,3- difluorobenzaldehyde under refluxing temperature followed by NaBH_4 reduction produced the compound **17a-b**. The series of compounds **18a-I** were synthesized by further functionalization of secondary nitrogen with various alkylating and various amide incurring groups.



Scheme 4. Synthetic Routes To Substituted Benzyl amines And 2,3-Difluoro Benzaldehyde Based Condensed Molecules **21a-f**

In continuation to these, we also aimed to prepare set of compounds by removing indole pharmacophore. In this regard, condensation of benzyl amine and 2,3-difluorobenzaldehyde was achieved in DCE at reflux condition followed by reduction with NaBH_4 in MeOH produced compounds **20a-b**. Further **20a-b** were treated with various amidating and sulfonylating agents for the synthesis of corresponding tert-amine derivatives **21b-f**.



Reagents and conditions: (i) benzyl amine, 2,3-difluoro benzaldehyde DCE reflux, NaBH₄, MeOH, 0 °C to rt 4 h.

Biological Activity: Screening Of Compounds For Anti-Adipogenic Activity In 3T3-L1 Preadipocytes

A series of compounds were screened for anti-adipogenic activity in 3T3-L1 cell line. The compound treatment was given along differentiation media and Oil-red O absorbance was taken at 492nm. The initial triazole/indole hybrid compounds synthesized **8a-f** (scheme 1) did not show any significant anti-adipogenic activity (Fig. 1A) (Supplementary table 1). Delightedly, 3-substituted indole and triazole molecules **13m-o** (Scheme 2) possessing 2,3-difluoro benzyl substitution on the triazole ring showed significant anti-adipogenic activity with 71, 39 and 31% of inhibition respectively (Fig. 1B) (Table 1). However, among the series of compounds **18a-l** (Scheme 3) containing indole as a pharmacophore **18a**, **18c**, **18g** and **18i** exhibited moderate anti-adipogenic activity with 45, 57, 21 and 25% of inhibition respectively (Fig. 1C) (Supplementary table 1). The decrease in anti-adipogenic activity in series of compound (**18a-l**) might be representing the pharmacophoric activity of triazole ring. Another series of compounds synthesized on the basis of SAR confirmed the essential functional groups necessary for the anti-adipogenic activity. Compounds in the fourth series **21a-f** (Scheme 4) showed non-significant anti-adipogenic activity (Fig. 2D).

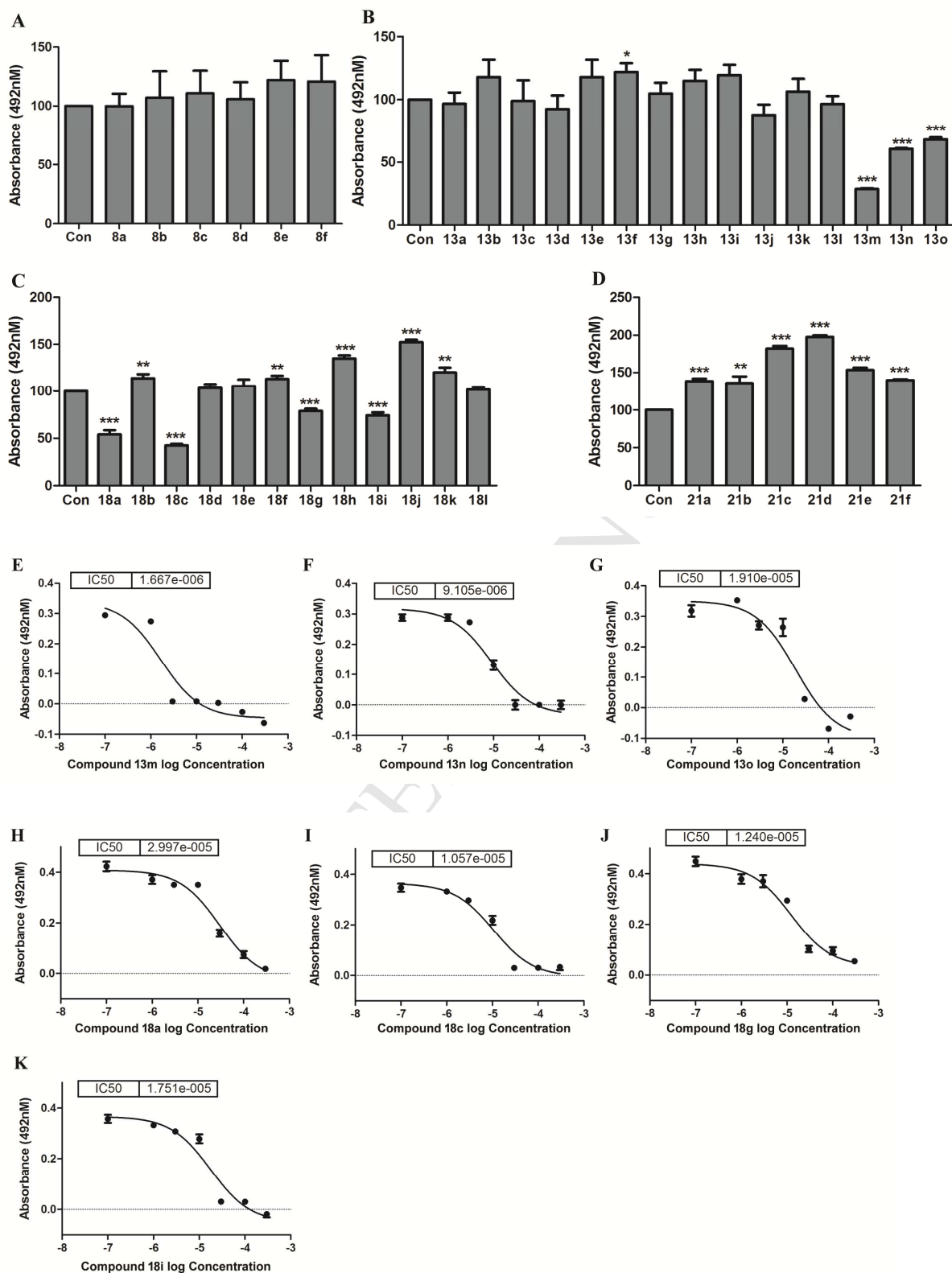


Figure 2. Screening Of Compounds For Anti-Adipogenic Activity In 3T3-L1 Preadipocytes

20 μ M of compound was given along with differentiation media in 3T3-L1 preadipocytes and stained with Oil red O. MDI+ was taken as control. The stain was collected and absorbance was taken at 492nm. n=3, error bars represent mean \pm SD. *p<0.05, **p<0.01, ***p<0.001 as tested by students *t* test. Significance is indicated in comparison to control (A-D). Log concentration dependent treatment of selected compounds in 3T3-L1 preadipocytes, n=3, error bars in the graph represent mean \pm SD (E-K). The actual concentrations used for treatment were 0.1, 1, 3, 10, 30, 100 and 300 μ M respectively which are converted to log concentration and analyzed in non-linear regression to find IC₅₀ value. The IC₅₀ values of the compounds are given in the box adjacent to the plot. The data are representative of three independent experiments.

Among all the triazole/indole hybrids, compounds **13m-o**, **18a**, **18c**, **18g** and **18i** exhibited maximum anti-adipogenic activity and were taken up for further study. Compound treatment was given in log concentration from 1 μ M to 300 μ M to calculate IC₅₀ value. IC₅₀ value of compound **13m-o**, **18a**, **18c**, **18g** and **18i** are given in table 1 (Fig. 2E-K).

Table 1: Molecular Weight And IC₅₀ Value Of Selected Compounds Based On Their Activity.

Compound Name	Molecular Weight	IC ₅₀ value (μ M)
13m	661.1629	1.7 \pm 0.8
13n	549.1646	9.1 \pm 0.9
13o	603.1364	19.1 \pm 3.4
18a	426.1214	30 \pm 5.5
18c	468.1319	17.5 \pm 2.2
18g	430.0963	12.4 \pm 0.7

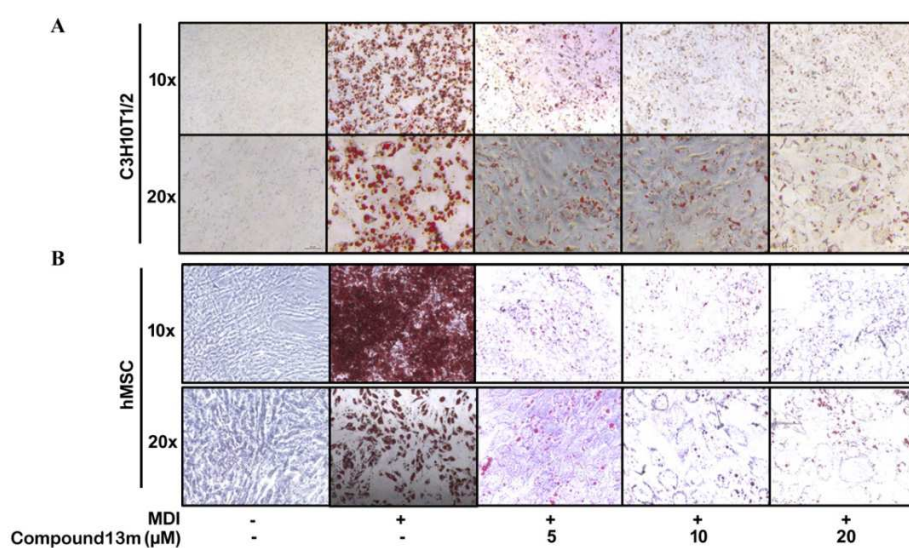
18i	472.1068	10.6 ± 3.1
------------	----------	------------

The IC₅₀ value calculated from two to three independent experiments is represented as mean ± SEM.

Among the selected compounds, **13m** showed most potent anti-adipogenic activity with IC₅₀ value of 1.67 μM and was selected for mechanistic study. Oil red O images of 3T3-L1 cells treated with lead compound **13m** at 5, 10 and 20 μM concentration were captured in imaging condition (Supplementary Fig. 1A). Compound **13m** did not show any cytotoxicity even at 100 times above the IC₅₀ concentration (Supplementary Fig. 1B). These results made us to choose the compound **13m** a suitable candidate for mechanistic study.

Anti-Adipogenic Activity Of Compound 13m In Different Cell Lines

Similar to above study, the anti-adipogenic activity of compound **13m** was checked in C3H10T1/2 and human mesenchymal stem cells (hMSC). As observed in 3T3-L1, both these cell lines when differentiated in presence of compound **13m** showed less lipid accumulation as seen in oil red O staining (Fig. 3A & B). The absorbance at 492nm of Oil-red O stain collected from lipid accumulated in C3H10T1/2 and hMSC indicated that the compound **13m** inhibits adipogenesis at various concentrations (5, 10, 20 μM) as shown in (Fig. 3C & D).



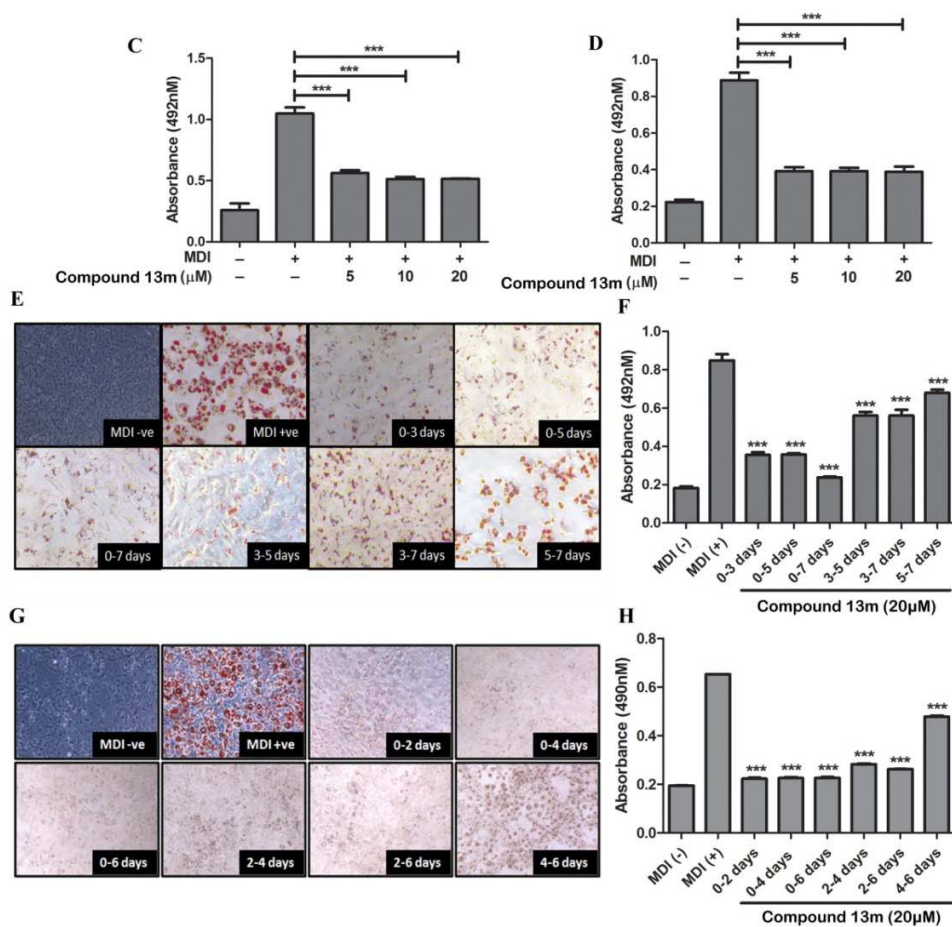


Figure 3. Anti-Adipogenic Activity Of Compound 13m In Different Cell Lines

Oil red O staining images of C3H10T1/2 and hMSC differentiated adipocytes treated with 5, 10 and $20\mu\text{M}$ respective concentration of compound **13m** along with differentiation media. The images were captured at 10x and 20x magnification with Leica microscope. The images are representative of three independent experiments. (A&B). Oil red O stain was collected from the lipid accumulated in C3H10T1/2 and hMSC differentiated adipocytes, absorbance was taken at 492nm, $n=3$, error bars represents mean \pm SD, $***p<0.001$ as tested by student t test. Significance is indicated in comparison to MDI+ group (C&D). Oil red O staining images of 3T3-L1 (E), C3H10T1/2 (G) differentiated adipocytes treated with $20\mu\text{M}$ of compound **13m** along with differentiation media for different time periods as given in figure (E and G). The images were captured at 10x magnification with Leica microscope, images are representative of three independent experiments (E&G). Oil red O stain was collected from the lipid accumulated in

3T3-L1 (F) and C3H10T1/2 (G) differentiated adipocytes, absorbance was taken at 492nm. n=3, error bars represents mean \pm SD, ***p<0.001 as tested by student *t* test. Significance is indicated in comparison to MDI+ group (**F&H**).

To further check the stage at which, the compound **13m** inhibits adipogenesis, day dependent compound treatment was given along with the differentiation media. The day dependent treatment of compound **13m** in 3T3-L1 cells during the period of differentiation showed maximum inhibition of adipogenesis at 0 to 7 days of treatment. The treatment of compound **13m** (20 μ M) at the early stage of differentiation (0-3days) was sufficient to significantly inhibit adipogenesis in 3T3-L1 cells (Fig. 3E & F). Similar to 3T3-L1, the compound **13m** inhibited adipogenesis at the early stage of differentiation in C3H10T1/2 cells (Fig. 3G & H). The above results indicate that the compound acts on the early stage of differentiation thereby inhibiting adipogenesis. This made us curious to investigate the action of compound **13m** in growth arrest and mitotic clonal expansion, the two early events in the process of adipogenesis.

Suppression of Mitotic Clonal Expansion By Compound 13m Via Activation of Wnt3a/ β catenin Pathway

To examine the effect of compound **13m** during mitotic clonal expansion, 3T3-L1 cells were incubated with 10 and 20 μ M of compound **13m** along with differentiation media for 16 and 24hr. After incubation period cell were fixed and cell cycle was analyzed using flow cytometry. Flow cytometry analysis indicated that MDI treatment leads to increased cell division and majority of cells are in S phase at 16hr times point, whereas in presence of compound **13m** the cells entering S phase was significantly reduced. At 24hr time point MDI treated cells were significantly less in

+S phase compared to cell treated with compound **13m**. The right panel besides the cell cycle

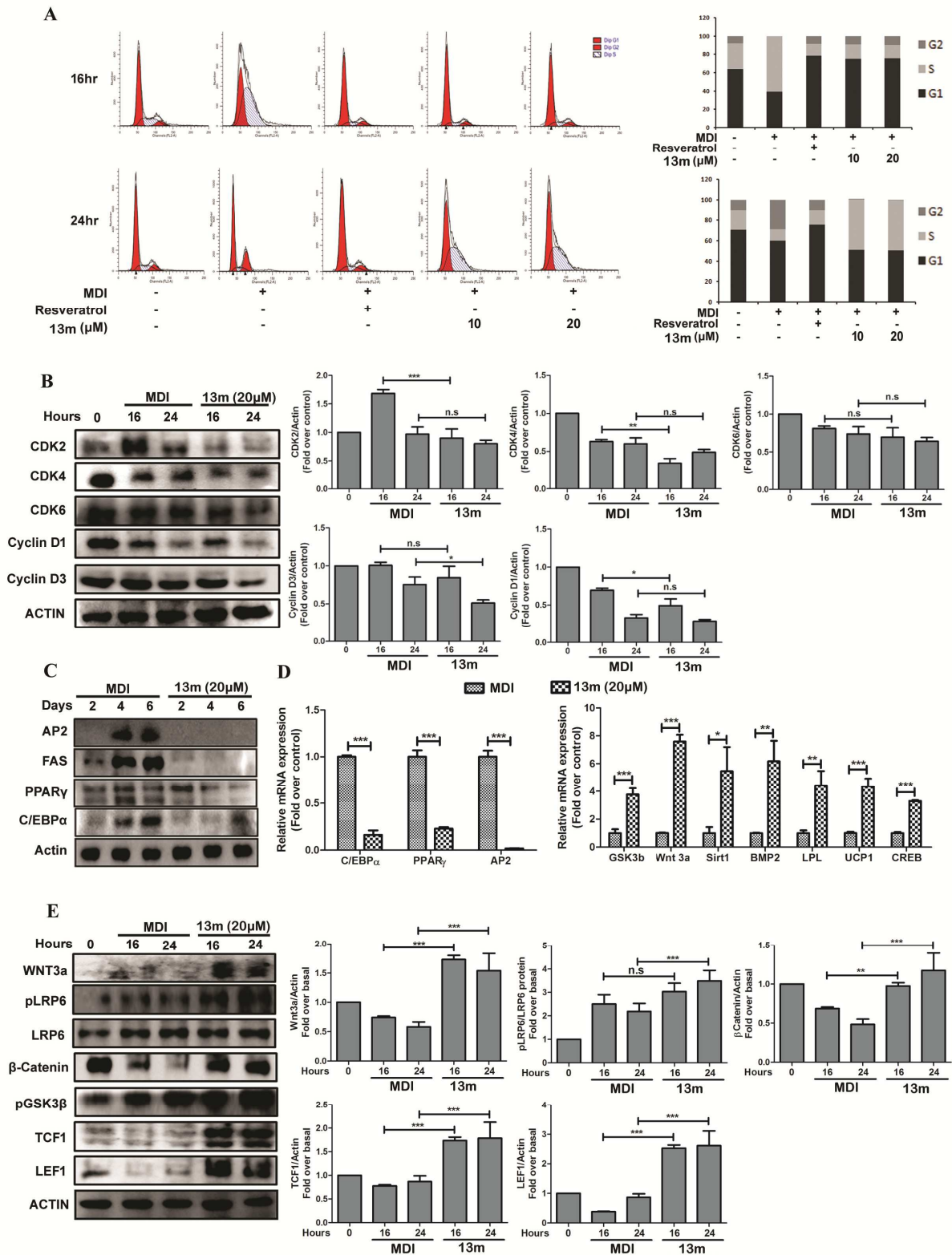


Figure: 4. Suppression of Mitotic Clonal Expansion By Compound 13m Via Activation of Wnt3a/ β catenin Pathway

3T3L1 adipocytes were exposed to compound **13m** (10 and 20 μ M) for 16 and 24hrs along differentiation media. Cells were fixed and stained with PI followed by cell cycle analysis using flow cytometry. 10,000 counts were taken in each reading. The data are representative of three independent experiments (**A**). 3T3-L1 cells were given MDI treatment with or without compound **13m** (20 μ M) and proteins were isolated at 16 and 24hrs. The isolated proteins were subjected to western blot analysis for proteins CDK2, CDK4, CDK6, CyclinD1 and CyclinD3. Actin was taken as loading control. Densitometry graphs normalized with actin are shown besides the blots. n=3, error bars represent mean \pm SD, *P<0.05, **P<0.01 and ***P<0.001 as tested by student *t* test (**B**). Western blot analysis of adipocyte specific proteins PPAR γ , C/EBP α , AP2 and FAS in MDI alone and with compound **13m** treated 3T3-L1 cells at different time points as given figure, n=3 (**C**). Real-Time PCR analysis of genes related to adipogenesis in 3T3-L1 cells treated with differentiation media with or without compound **13m** (20 μ M) during the period of differentiation. n=3, error bars represent SD, *P<0.05, **P<0.01, ***P<0.001 as tested by one way ANOVA and Bonferroni post-test analysis (**D**). 3T3L1 cells were given MDI treatment with or without compound **13m** (20 μ M) and protein were isolated at different time points as given in the figure. The isolated proteins were subjected to western blot analysis for following proteins Wnt3a, pLRP6, β catenin, pGSK3 β , TCF1 and LEF1. The densitometry analysis of above mentions proteins normalized with either Actin or their respective proteins is given besides the blot. n=3, error bars represent SD, *P<0.05, **P<0.01 and ***P<0.001 as tested by one way ANOVA and Bonferroni post-test analysis (**E**). All results are representative of three independent experiments.

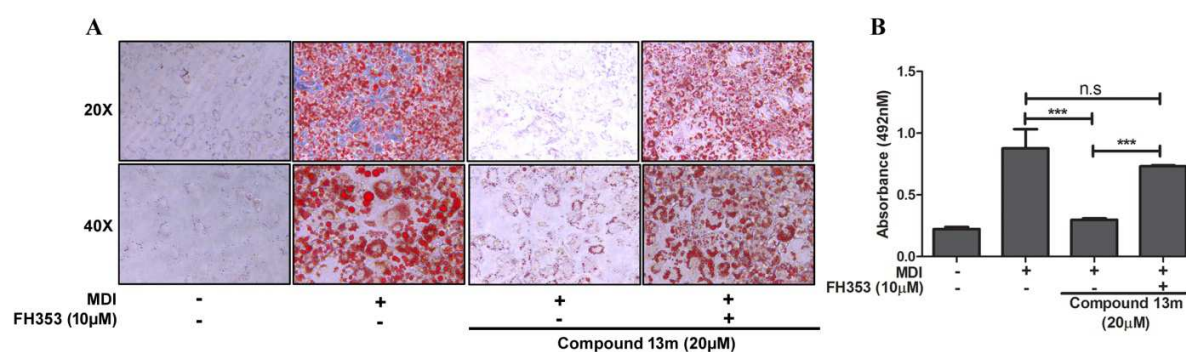
analysis graph shows the percentage of cells in different phase of cell cycle (Fig. 4A). Further study of proteins involved in cell cycle show that compound **13m** particularly blocks G1 to S phase transition as commitment to enter S phase occurs through sequential phosphorylation of

Rb by CyclinD CDK4/CDK6 and CyclinE/CDK2 proteins[36] which were found to be down regulated at 16hr and 24hr time point in compound **13m** treated cells (Fig.4B). The above result together with cell cycle analysis study confirms the G1 to S phase cell cycle arrest by compound **13m**. The mRNA expression profile of 3T3L1 cells treated with compound **13m** showed decreased expression of adipogenic transcription factors PPAR γ , C/EBP α and AP2 gene as well as increased expression of Wnt3a, BMP2 (Bone morphogenetic protein 2), SIRT1 (sirtuin-1), CREB (cAMP response building proteins) compared to control cells (Fig. 4C). We did not find increased expression of other Wnt family members such as Wnt5a, Wnt5b, Wnt10a which are known to inhibit adipogenesis (Supplementary Fig. 2A) Among the aforementioned genes, PPAR γ , C/EBP α , AP2 and FAS were validated at protein level and were found to be decreased in compound **13m** treated 3T3L1 cells at different time intervals (Fig. 4D). The clues obtained from above results suggest the involvement of proteins associated with Wnt3a pathway at 16 and 24 hr time point.

The compound **13m** showed increased expression of Wnt3a at the protein level as well. As expected the downstream proteins of Wnt3a pathway, LRP6 and β -Catenine were found to be activated (increased phosphorylation) in compound **13m** treated cells. The treatment of compound **13m** on 3T3L1 adipocytes also led to increased expression of TCF1 and LEF1 at 16 and 24 hr time point (Fig. 4E). TCF1 and LEF1 are known to suppress PPAR γ , C/EBP α and other pro-adipogenic genes [37] [38]. From the above results, it can be concluded that the one of the possible mechanisms by which compound **13m** inhibit adipogenesis is by arresting cell cycle, which might be in turn due to activation of Wnt3a/ β -catenin pathway.

Inhibition Of β -Catenin/TCF Pathway By FH353 Abolishes Anti-Adipogenic Activity Of The Compound 13m

To validate that anti-adipogenic activity of the compound **13m** is mediated by Wnt3a/ β -catenin pathway, We used FH353 which is an inhibitor of β -catenin/TCF complex [39]. 3T3L1 pre adipocytes on treatment with the compound 13m in presence of FH353 (10 μ M) differentiated to adipocytes on MDI treatment, similar to control cells (Fig. 5A and B). Cell cycle analysis showed that the compound **13m** failed to arrest G1/S phase transition in presence of FH353 at 24hr time point on treatment with MDI (Fig. 5C). Further analysis of proteins involved in cell cycle regulation at 16 and 24 hr time point showed that in presence of FH353 the compound **13m** treated cell showed increased expression of CDK2, CDK4, CDK6, cyclinD1 and cyclinD3 similar to control cells and failed to activate β -catenin/TCF proteins (Fig. 5D and E). Moreover, in presence of FH353 3T3L1 cell showed increased expression of PPAR γ , C/EBP α , FAS and AP2 similar to control cells on treatment with compound **13m**. The above results confirm that the compound 13m inhibits adipogenesis by wnt3a/ β -catenin pathway.



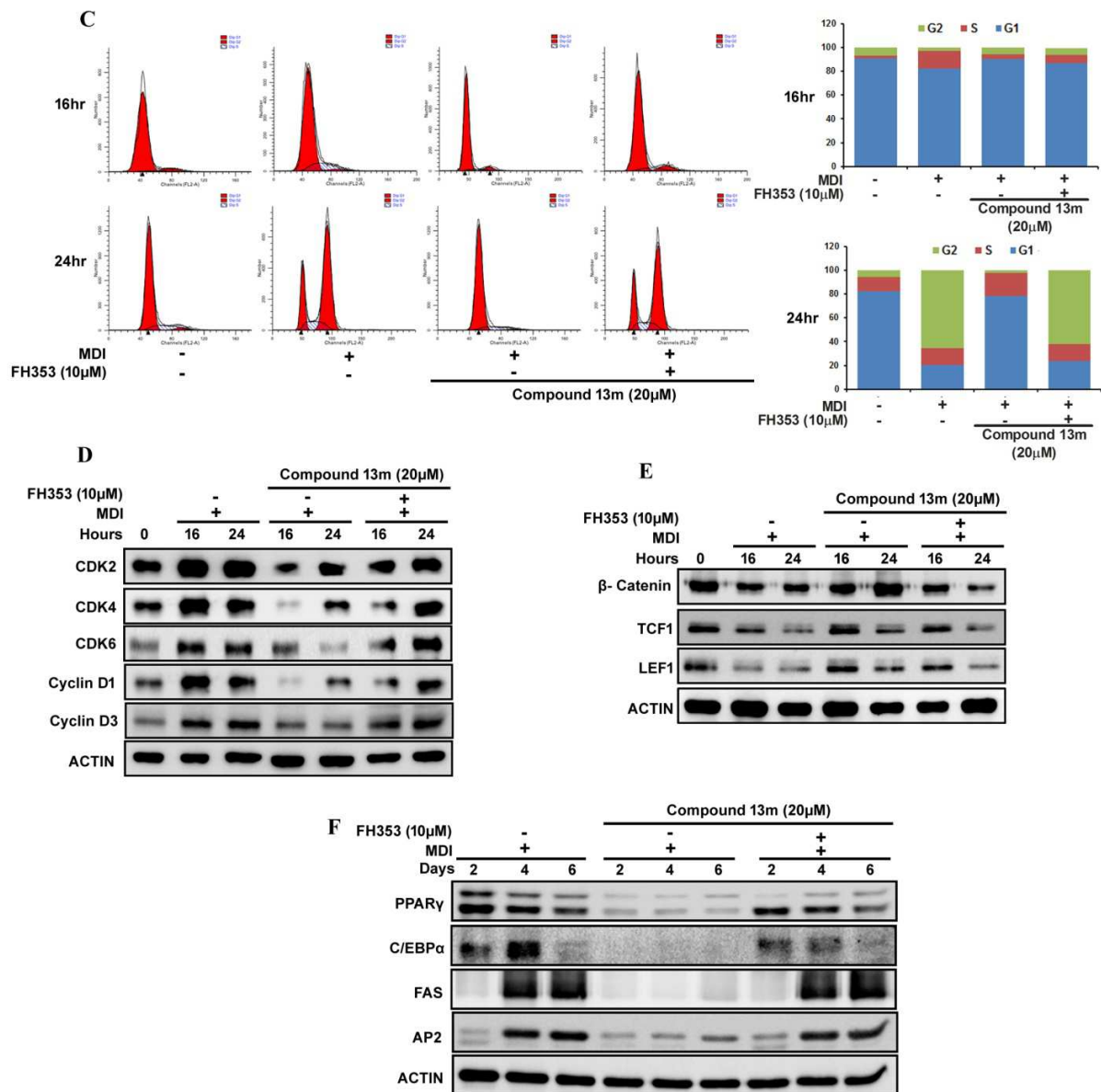


Figure 5: Inhibition Of β -Catenin/TCF Pathway By FH353 Abolishes Anti-Adipogenic Activity Of The Compound 13m

Oil red O staining images of 3T3L1 adipocytes treated with the compound **13m** (20 μ M) with or without FH353 (10 μ M) along with differentiation media. The images were captured at 20x and 40x magnification with Leica microscope. The images are representative of three independent experiments. (A). Oil red O stain was collected from the lipid accumulated in C3H10T1/2 and hMSC differentiated adipocytes, absorbance was taken at 492nm. n=3, error bars represents mean \pm SD, ***p<0.001 as tested by student *t*

test (B). 3T3L1 adipocytes were exposed to compound **13m** (20 μ M) for 16 and 24 hrs along differentiation media with or without FH353 (10 μ M). Cells were fixed and stained with PI followed by cell cycle analysis using flow cytometry. 10,000 counts were taken in each reading. The data are representative of three independent experiments (C). 3T3-L1 cells were treated with compound **13m** (20 μ M) with or without FH353 (10 μ M) and proteins were isolated at 16 and 24hrs. The isolated proteins were subjected to western blot analysis for proteins involved in cell cycle regulation, β -catenin, TCF-1 and LEF1 (D and E). Actin was taken as loading control. n=3. 3T3L1 cells were differentiated in presence of compound 13m (20 μ M) or FH353 (10 μ M) using MDI as shown in Figure (F). Proteins were isolated at 2, 4 and 6th day and subjected to western blot analysis for PPAR γ , C/EBP α , FAS and AP2. Actin was used as loading control. n=3 (F).

Compound 13m Ameliorates Dyslipidemia in Syrian Golden Hamster Model

Many naturally occurring anti-adipogenic compound such as curcumin and berberine are also known to improve dyslipidemia [40][41]. Moreover our own previous studies indicate that anti-adipogenic compounds also exhibits antidyslipidemic activity [42][6][43]. On this basis, the anti-dyslipidemic potential of compound **13m** was investigated in Syrian Golden hamster model for dyslipidemia, which serves as a standard *in vivo* model [44]. In the course of study, 7 days compound **13m** treatment ameliorated serum lipid profile evaluated by significant reduction of serum TG, TC LDL and NEFA levels compared to dyslipidemic group (Fig. 6A-D). We did not found significance HDL level alterations in the treatment group (Fig. 6E). However, we find a significant attenuated atherogenic index (TG/HDLc ratio) in the compound treated group (Fig. 6F). In addition, compound **13m** treatment significantly attenuated serum ALT (Figure5G) level and relatively decreased AST level (Fig. 6H) as compared to HFD fed group indicating that the compound is not hepatotoxic and has beneficial effect. Western blot analysis showed increased

β -catenin and decreased PPAR γ protein level in the eWAT of compound treated group (Fig. 6I) which further support the anti-adipogenic potential of the compound observed in *in vitro* studies.

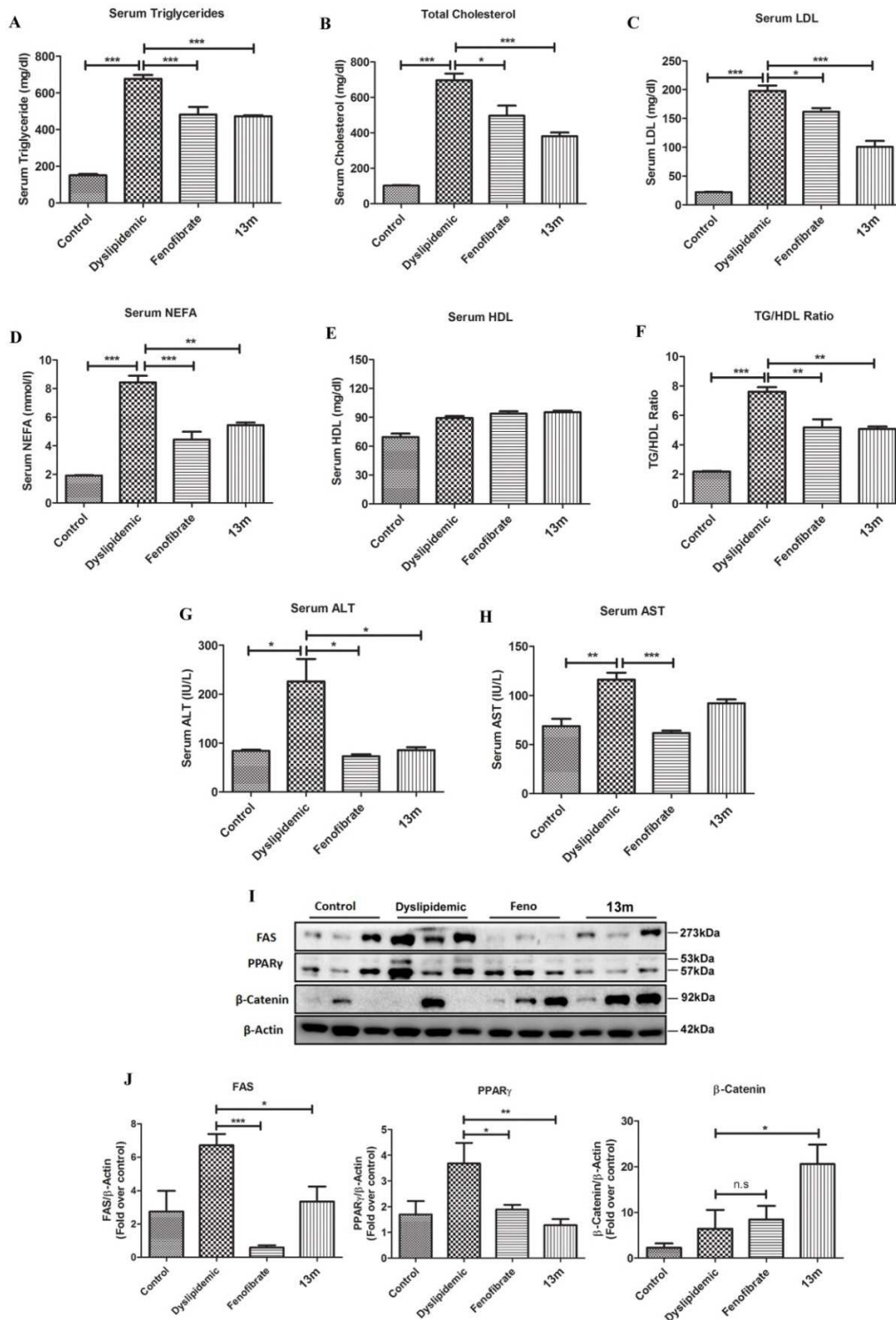


Figure 6. Compound 13m Ameliorates HFD Induced Dyslipidemia In The Syrian Golden Hamster Model

HFD fed hamsters showed dysregulated serum lipid profile. 7days treatment of compound **13m** significantly attenuated serum triglycerides (TGs) (A), total cholesterol (TC) (B), LDL (C) and NEFA (D) levels as compared to HFD fed group. Compound **13m** treatment did not alter serum HDL-c levels significantly (E); while the compound **13m** significantly attenuates TG/HDL-c ratio (F), a marker for atherogenic index. Compound **13m** significantly attenuates serum ALT (Alanine Transaminase) as compared HFD fed group (G), AST (Aspartate Transaminase) level was non-significant among all groups (H). All data are expressed in mean \pm SEM (n=4 hamster per group). Statistical significance was measured by one way ANOVA followed by Bonferroni posttest analysis. Statistical significance denoted by *p<0.05, **p<0.01, ***p<0.001. n.s. means non-significant difference between groups. Proteins isolated from epididymal white adipose tissue (eWAT) were subjected to western blots of denoted proteins in different groups (I), error bars represent mean \pm SD of three independent experiments. *P<0.05, **P<0.01, ***P<0.001 as tested by one way ANOVA followed by Bonferroni posttest analysis. All results are representative of three independent experiments.

Compound 13m Regulates Lipid Metabolism by Promoting Reverse Cholesterol Transport (RCT)

As high-fat diet-induced dyslipidemia is known to impair RCT[45], hepatic genes associated with lipid metabolism were analyzed to understand the mode of action of compound **13m**. Comparative gene expression analysis showed significant increase in the expression of genes such as PPAR α (peroxisome proliferator-activated receptor α), LXR1 α (Liver X receptor 1 α), HNF1 α (Hepatocyte nuclear factor 1 α) and ApoA (Apolipoprotein A) in liver of the compound **13m** treated group (Fig. 7A). Among them, PPAR α and LXR1 α are the two major genes elevated following compound **13m** treatment and both play a key role in RCT.[46] Therefore, further studies on adipose and hepatic genes associated with RCT were performed.

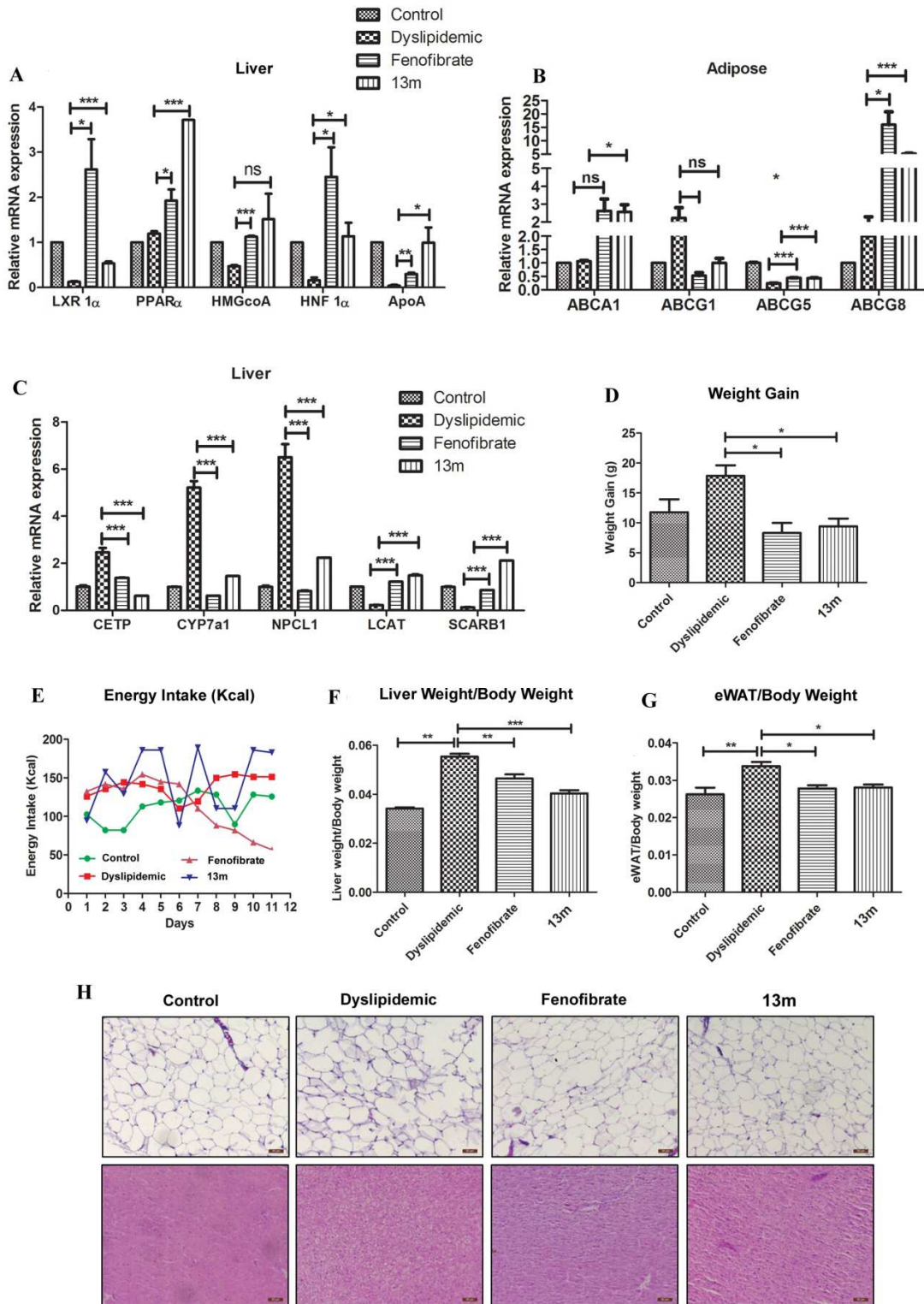


Figure: 7. Compound 13m Regulates Lipid Metabolism by Promoting Reverse Cholesterol Transport (RCT).

Comparative gene expression analysis of denoted key genes involved in hepatic lipid metabolism was up-regulated in liver after compound **13m** treatment, n=3, error bars represent mean \pm SD, (A). RCT related genes in eWAT showed similar results in **13m** treated group compared to positive control fenofibrate (B). RCT related genes in liver showed similar results in **13m** treated group compared to positive control fenofibrate (C). Compound **13m** treatment group showed less weight gain as compared to all groups (D). Compound **13m** treatment did not show significant change in energy intake from HFD feeding (E). Compound **13m** significantly attenuated liver weight/total body weight as compared to HFD fed group (F). Compound **13m** attenuated eWAT/body weight as compared to HFD fed group (G). H&E staining showed decreased adipocyte hypertrophy and hepatic lipid vacuoles in compound **13m** treatment group (H). All data were expressed in mean \pm SEM except hepatic mRNA expression (mean \pm SD). Statistical significance denoted by * p <0.05, ** p <0.01, *** p <0.001. All results are representative of three independent experiments.

In this cohort, compound treatment showed increased expression of reverse cholesterol transport genes ABCA1, ABCG8 and ABCG5 in adipose tissue similar to fenofibrate (Fig. 7B).

In addition, compound **13m** showed decreased expression of CETP, CYP7a1, NPCL1 and increased expression of SCARB1 and LCAT genes in liver similar to standard compound fenofibrate (Fig. 7C). The comparative gene expression studies indicated that compound **13m** improves dyslipidemia by promoting RCT. The compound **13m** treated animals gained significantly lesser weight compared to the dyslipidemic group (Fig. 7D). However non-significant patterns in energy intake were observed among all groups (Fig. 7E). Interestingly, compound treated animals had significantly lower liver and eWAT/body weight (Fig. 7F & G). H&E staining showed decreased adipocyte hypertrophy and hepatic lipid vacuoles in compound

13m treated group (Fig. 7H). The *in vivo* study validates the *in vitro* findings and shows that apart from inhibiting adipogenesis, the compound **13m** also improves dyslipidemia by activating RCT in FHD fed Syrian Golden hamster.

Table: 2 Primer sequences of genes analyzed by qRT-PCR in 3T3L1 preadipocytes.

Gene	Primer sequence
Fabp4 Forward	GCAGTGTTTCTGTGGCTGACAC
Fabp4 Reverse	GCCATGCACAGGGTCCA
PPAR γ Forward	GATTCACTTTTCTGGGACTGA
PPAR γ Reverse	GCCACTGTGCCGTACAGAGA
C/EBP α Forward	GGCCAATGGCATCCAAAATA
C/EBP α Reverse	CCTTGCGAATTCTGTGAGC
Wnt3a Forward	TGCTGTCCCTGTATGCCTCTG
Wnt3a Reverse	AGGGAGAGCGTAGCCCTCAT
Gsk3 β Forward	TCATCAGGACAACGCGATTTAAGAA
Gsk3 β Reverse	GCAGTCGGACTATGTTACAGTGG
LPL Forward	TCAGCATCTTCTCTGCAGACCGG
LPL Reverse	TCATTAGCATCCGTGGGAACA
Ucp 1 Forward	GGCCTCTACGACTCAGTCCA
Ucp 1 Reverse	TAAGCCGGCTGAGATCTTGT
SIRT1 Forward	CCTCCATGCCTGACTAAAGG
SIRT1 Reverse	TGAAATTCCAGCACTTTGGA
BMP2 Forward	GAGGCGAAGAAAAGCAACAG
BMP2 Reverse	CTCCACATGGAAAAAGCTCTG

CREB Forward	CAGGCAGGTGTTTCACAGG
CREB Reverse	GCATGTTTCAGAGGGTTAGGG
18s RNA Forward	GCCGCTAGAGGTGAAATTCTT
18s RNA Reverse	CGTCTTCGAACCTCCGACT

Adipogenesis is driven by a complex cascade of transcriptional factors leading to the sequential development of preadipocyte into mature adipocyte.[47] At the molecular level, PPAR γ activation is sufficient enough to trigger the process of adipogenesis and arrest the growth of preadipocytes compelling them to enter mitotic clonal expansion.[48, 49] PPAR γ is in turn activated by C/EBP α and is necessary for the continuous maintenance of PPAR γ expression. The compound **13m** decreases the expression of both C/EBP α and PPAR γ after differentiation media induction (MDI-Media containing 3-Isobutyl-1-methylxanthine (500 μ M), insulin (5 μ g/ml) and dexamethasone (250nM). During the early stage of adipogenesis, cells retract from their normal growth and undergo MCE (mitotic clonal expansion), which is composed of at least two rounds of cell division [50]. MCE is considered to be a necessary step in the event leading to adipogenesis and the cells which do not undergo MCE do not differentiate into adipocytes [50]. Compound **13m** inhibits mitotic clonal expansion as evident from the cell cycle experiment. The doubling time of 3T3-L1 adipocytes is around 24hr and they undergo MCE within first 2 days of MDI treatment [41]. As observed in flow cytometry experiment, the compound **13m** treated 3T3-L1 cells were significantly less in S phase compared to control after 16hr of MDI induction. This indicates that control cell after 16hrs of MDI induction undergoes mitotic clonal expansion. Similar to compound **13m**, many anti-adipogenic compounds such as resveratrol have shown to inhibit G1 to S phase transition [51]. Resveratrol is also known to activate β -catenin pathway

hence we used resveratrol as positive control in cell cycle regulation experiment [52-54]. One of the key observations was the increased expression of Wnt3a, which is known to regulate cell proliferation and differentiation [55]. Different cell lines are available to study adipogenesis, but each of these capture only specific mechanistic aspect of adipogenesis. Recently, the necessity of MCE for adipogenesis has been a matter of debate as human mesenchymal stem cells have been shown to differentiate into adipocytes without undergoing MCE [56]. To check whether the compound **13m** shows similar anti-adipogenic potency in different adipogenesis model and to rule out species specificity, we tested the compound in C3H10T1/2 and hMSC cell lines. The compound showed similar anti-adipogenic potency in all cell lines irrespective of their origin.

Wnt family members are glycoproteins, which act on the frizzled receptors responsible for the maintenance of β -catenin. Although the Wnt pathway is known to inhibit adipogenesis by both β -catenin dependent and independent pathway, more emphasis has been recently given to canonical pathway[57, 58]

Table: 3 Prime sequences of genes analyzed by qRT-PCR in hamster

Gene	Primer sequence
<i>Lxra Forward</i>	TCAGCATCTTCTCTGCAGACCGG
<i>Lxra Reverse</i>	TCATTAGCATCCGTGGGAACA
<i>HMGCR Forward</i>	GAGCTACATTTGTGCTTGGCG
<i>HMGCR Reverse</i>	TTCATTAGGCCGAGGGCTCAC
<i>LPL Forward</i>	GATTCACCTTTCTGGGACTGA
<i>LPL Reverse</i>	GCCAACTGTGCCGTACAGAGA
<i>PPARα Forward</i>	GGCCAATGGCATCCAAAATA
<i>PPARα Reverse</i>	CCTTGCGAATTCTGTTGAGC

<i>β-Actin Forward</i>	TGCTGTCCTGTATGCCTCTG
<i>β-Actin Reverse</i>	AGGGAGAGCCTAGCCCTCAT
<i>ApoA1 Forward</i>	ACCGTTCAGGATGAAAAGTGTAG
<i>ApoA1 Reverse</i>	GTGACTCAGGAGTTGCTGGGATAAC
<i>LCAT Forward</i>	CACACAAGGCCTGTCATCCT
<i>LCAT Reverse</i>	AGCACAACCAGTTCACCACA
<i>SREBP1c Forward</i>	GCAAGGTGTTCTGCATGAA
<i>SREBP1c Reverse</i>	TGGTGTCTGACTGGTACGCC
<i>ABCA1 Forward</i>	ATAGCAGGCTCCAACCTGAC
<i>ABCA1 Reverse</i>	GGTACTGAAGCATGTTTCGATGTT
<i>ABCG1 Forward</i>	GCCTGGTGACACAGACTCTC
<i>ABCG1 Reverse</i>	CAAACAGTTCACCCGGTG
<i>ABCG5 Forward</i>	TGATTGGCAGCTATAATTTTGGG
<i>ABCG5 Reverse</i>	GTTGGGCTGCGATGGAAA
<i>ABCG8 Forward</i>	TGCTGGCCATCATAGGGAG
<i>ABCG8 Reverse</i>	TCCTGATTTTCATCTTGCCACC
<i>CETP Forward</i>	AAGGGTGTGTCGTGGTCAGTTCT
<i>CETP Reverse</i>	ACTGATGATCTCGGGGTTGAT
<i>CYP7A1 Forward</i>	CACTCTGCACCTGAGGATGG
<i>CYP7A1 Reverse</i>	GGTCTGGGTAGATTGCAGG
<i>NPC1L1 Forward</i>	CCTGACCTTTATAGAACTCACCACAGA
<i>NPC1L1 Reverse</i>	GGGCCAAAATGCTCGTCAT

In canonical Wnt pathway, β -catenin plays a central role in the inhibition of adipogenesis. Wnt3a on binding with frizzled receptor or low-density lipo-protein receptors (LRPs) stabilizes β -catenin and translocate it from the cytoplasm to nucleus.[59] The accumulation of β -catenin inside the nucleus leads to activation of TCF/LEF transcription factors, which inhibit the expression of genes related to adipogenesis. 3T3-L1preadipocytes have high expression of β -catenin [60]. The interaction between Wnt3a with the frizzled receptor is necessary for the maintenance of the preadipocytes in the undifferentiated state; hence 3T3-L1preadipocytes have high expression of β -catenin as observed in 3T3-L1 preadipocyte sample (Fig. 4E). The compound **13m** treatment with differentiation media increased expression of the proteins involved in canonical Wnt3a/ β -catenin pathway and increased the expression of TCF1 and LEF1 transcription factors. These transcription factors are known to inhibit the expression of PPAR γ and C/EBP α as observed in the result. One of the interesting observations is the increased expression of PPAR α in the liver of compound treated mice. The study conducted by Gedaly R *et al.*, showed that activation of Wnt3a/ β -catenin pathway did not alter the expression of PPAR α in liver cells [39] Recent reports and literature evidence clearly indicate negative correlation between wnt3a/ β -catenin pathway and PPAR γ [61] but its effect on PPAR α remains ambiguous.

The *in vitro* studies conducted on 3T3L1 preadipocytes revealed the potential effects of compound **13m** on lipid metabolism. Further to investigate compound **13m** *in vivo* potential, hamster model of high-fat diet-induced dyslipidemia was used. As many naturally occurring anti-adipogenic compound such as curcumin and berberine are also known to improve dyslipidemia [40, 41]. Moreover our own previous studies indicate that anti-adipogenic compounds also exhibits antidyslipidemic activity [6, 42]. Interestingly, compound **13m**

treatment for one week showed improved serum lipid profile. Decreased adipogenic marker PPAR γ and increased anti-adipogenic marker β -catenin [62, 63] at the protein level in eWAT of compound **13m** treated hamster further validates the *in vitro* findings. To identify the possible mechanism responsible for the anti-dyslipidemic activity of the compound, we did hepatic gene expression analysis of the key genes that regulate lipid metabolism. Compound **13m** treatment led to increased expression of PPAR α and LXR1 α genes, which are known to activate RCT [46]. Therefore, further RCT pathway analysis was done by taking fenofibrate as the positive control [64-66]. All the above results affirm that compound **13m** showed improved lipid profile by activating the PPAR α -LXR1 α -RCT pathway.

Conclusion

To summarize, in this study we have evaluated anti-adipogenic activity of triazole and indole hybrid compounds. We have identified functional groups essential to potentiate the anti-adipogenic activity and optimized the lead compound **13m** based on SAR. Compound **13m** inhibit adipogenesis at very early stage and arrest G1/S phase cell cycle transition by activating Wnt3a/ β -catenin pathway. The *in vitro* findings have been validated in Syrian Golden hamster diet induced dyslipidemia model. *In vivo* studies also suggest RCT as one of the possible mechanism responsible for the dyslipidmic activity of compound **13m**. Overall this study gives a unique perspective in to anti-adipogenic/anti-dyslipidemic property of triazole/indole hybrids with further scope to improve potency of compounds for therapeutic interventions in obesity and metabolic syndrome.

Materials and Methods

Differentiation Of 3T3-L1, C3H10T1/2 And Human Mesenchymal Stem Cell

The 3T3-L1, C3H10T1/2 cell lines were purchased from the American Type Culture Collection (Manassas, VA). Cells were cultured in humidified atmosphere containing 5% CO₂ at 37°C. High glucose Dulbecco's modified Eagles Medium (DMEM) (GIBCO Grand Island, NY) supplement with 10% heat inactivated fetal bovine serum and penicillin streptomycin antibiotics (Invitrogen, Carlsbad, CA) was used for culture. For adipogenic differentiation, 50,000/well were seeded in 24 well plates. Two days after reaching confluence, cells were given differentiation media (media containing 0.5mM 3-isobutyl-1- methylxanthine, 5µg/ml insulin and 250nM dexamethasone). The differentiation media was replaced with media containing insulin 5µg/ml at third day of treatment. After 48hrs incubation media containing insulin was replaced with complete media. More than 90% of cells contained lipid droplets after complete induction of differentiation.

Bone marrow derived human mesenchymal stem cell (hMSC) was purchased from Stempeutics Research Pvt Ltd (Bangalore). MSC was differentiated using a cocktail containing 500µM IBMX, 5µg/ml insulin, 1µM dexamethasone and 200µM indomethacin. Cells were maintained in differentiation cocktail containing media for 9 days and media was changed every third day. Differentiation media was replaced with media containing insulin 5µg/ml and maintained for 3 days. Fully differentiated adipocytes were maintained in complete media thereafter.

Cell Viability Assay

MTT assay: 3T3-L1 cells were seeded in 96 well plate at a density of 1×10^4 cells per well. Cells were allowed to grow in complete media for 24hrs. Cells were then treated with various concentrations (1 µM to 1000 µM) of compound **13m**. After 24hrs media containing compound **13m** was removed and cells were incubated for 3hrs with media containing MTT at a concentration of 0.5µg/ml. The supernatant was aspirated and DMSO was added to each well.

Absorbance was taken at 570 nm using multi-well plate reader. The result is representative of three independent experiments. The result given is the representative of three independent experiments. Error bars in the graph represent mean \pm SD.

Oil red O Staining

Oil red O staining was performed as previously described[6]. Briefly, differentiated 3T3-L1 adipocytes (with or without compound **13m**) were washed with PBS (pH 7.4) and incubated with Oil red O (0.36% ORO in 60% isopropanol) for 20mins. The Oil red O from the stained lipid droplet was extracted using 100% isopropanol and absorbance was taken at 492nm. The values are expressed as the mean of three independent experiments and error bars represent mean \pm SD. Significance was assessed by student *t* test.

Western Blotting

Protein lysate of cells (with or without compound **13m** treatment) were prepared by using ice cold mammalian cell lysis buffer containing protease and phosphatase inhibitor (Roche). Protein concentration was measured using Bicinchoninic Acid assay (BCA) method. Equal quantity of protein was taken for sample preparation. Protein samples were denatured and supplemented with 10% β -mercaptoethanol. Protein samples were resolved in 8 to 12% SDS-PAGE and electro-transferred to nitrocellulose membrane at 50V for 2hrs. 5% skimmed milk (Sigma) in tris-buffered saline containing 0.05% Tween-20 (TBS-T) was used for blocking the membrane. Membrane was washed with TBST and incubated overnight with target protein specific antibodies at 4°C for overnight. Next day Membrane was incubated with HRP conjugated secondary antibody for 1hr and the target protein was detected using chemi-luminescence detector (Millipore; Billerica, USA) on Image Quant LAS 4000. β -actin was used as an internal control. The blots presented are representative of three independent experiments. Error bars

represent mean \pm SD unless otherwise stated in figure legend. Statistical significance was assessed by either one way ANNOVA followed by Bonferroni posttest analysis or student t test as mentioned in figure legends.

Cell Cycle Analysis Using Flow Cytometry

3T3-L1 preadipocytes were cultured in T25 flask till confluence. Cells were incubated with differentiation media with or with compound **13m** (concentration $10\mu\text{M}$ and $20\mu\text{M}$) for 16 and 24hr. The cell were washed with PBS and trypsinized. The cell pellet was washed with 1 ml PBS and fixed in 70% ice cold ethanol for 2hr. the cells were pelleted and re-suspended in propidium iodide solution ($40\mu\text{g/ml}$ in RNAaseA containing buffer) for 30mins at room temperature. Minimum 20,000 events were acquired per sample on flow cytometer (FACS Calibur, BD). The data was analyzed using Modfit software to determine the relative number of cells in G1, S and G2/M phase. The result is representative of three independent experiments.

Quantitative Real-Time RT-PCR

Cells were thoroughly washed with PBS and RNA was isolated using TRIZOL reagent (Invitrogen CA, USA). Quantification of RNA was done by Nanodrop 2000c (Thermo Fisher Scientific India Pvt. Ltd.) and 500ng of RNA was used for cDNA preparation. cDNA was synthesized using high capacity cDNA reverse transcription kit (Applied Biosystems, Foster City, CA, USA). Quantitative real time PCR was performed using SYBR Green master mix on Light Cycler 480 (Roche Diagnostics). Relative change in gene expression was normalized with endogenous reference gene 18S rRNA for 3T3L1 preadipocytes and β -actin for hamster. Change in gene expression was calculated by ($2^{-\Delta Ct}$) method. The primer list of the analyzed genes is given in Table 3 and 4. The values are expressed as mean of three independent experiments each containing triplicate values. The error bars in the graph represent mean \pm SD unless and

otherwise mentioned in figure legend. The significance is calculated by one way ANNOVA followed by Bonfferoni posttest analysis.

Animal Experiments And Diet Interventions

For *in vivo* evaluation of the compound, we used Syrian Golden hamster (male, 8-10 weeks old and 100-120g body weight range) provided by laboratory animal facility (LAF), CSIR-CDRI, Lucknow. All the protocols were approved by institutional animal ethical committee (IAEC), CSIR-CDRI, Lucknow as per CPCSEA guidelines (Approval number: IAEC/2013/02/Renewal 02 (63/15) Throughout the study animals were housed in polypropylene cages (4 animals per cage) kept on well controlled environment of $25\pm 1^{\circ}\text{C}$, 45-55% RH and a 12:12 light/dark cycle. Animals were fed with normal chow diet and/or 45% kCal high fat diet (Cat. No D12451, Research Diets Inc) and water ad libitum.

Treatment Schedule and Sample Collection

At first animals were acclimatized for one week and then randomized in four groups (4 hamsters per group). Among these, first group was kept on normal chow diet (control group) and the rest 3 groups were kept on HFD for 4 days. From fifth day onwards, the first group continued on normal chow diet and vehicle (p.o.), second dyslipidemic group received HFD and vehicle (0.5% w/v NaCMC, (Carboxymethyl Cellulose sodium salt brought from Sigma Aldrich #419273), whereas third and fourth group received HFD with positive control fenofibrate (100mg/kg, p.o.) and compound **13m** (100mg/kg, p.o.) respectively for one week. Routine animal monitoring like food intake and body weight were done at scheduled morning time, daily. After one week of treatment schedule hamsters were fasted overnight, blood was collected from retro-orbital plexus under anesthesia and processed for serum separation. At the end animals were sacrificed under

deep anesthesia, perfused with normal saline, tissues (Liver and eWAT) were dissected out, weighed and processed as per the need of subjected techniques or stored at -80°C .

Serum Analysis and Histology

Serum total cholesterol (TC), HDL cholesterol, LDL cholesterol, Triglycerides (TG), glucose, ALT and AST were estimated by using Cobas Integra 400TM Clinical Bio-analyzer (Roche Diagnostics). NEFA were measured by using kit from Randox laboratories as per given instructions. Haematoxylin and eosin (H&E) staining in liver and eWAT paraffin embedded sections were done by de-paraffinization in xylene followed by rehydration in gradient alcohol. Images were taken in Leica bright field microscope at 20x magnification.

Statistical Analysis

All the data are expressed as mean \pm SD otherwise mentioned in the figure legend. Student T test was used to calculate statistical significance. Comparison between treated and control groups were performed by one way analysis of variance (ANOVA) followed by Bonferroni's multiple comparison test. Graph Pad Prism. IC_{50} was calculated by non-linear regression curve, where actual concentrations are converted to logarithmic value and plotted in log inhibitor verse response curve (Version 7, Graph Pad Software Inc. Sandiego, CA, and USA) was used to analyze data. $p < 0.05$ was used as the criteria for statistical significance.

Article Information

Funding:

Research work is supported by CSIR-CDRI Network project: "Towards holistic understanding of complex diseases: Unraveling the threads of complex disease (THUNDER) Project No: BSC0102.

Conflict Of Interest Statement

The authors declare that they have no conflicts of interest with the contents of this article.

Acknowledgment

We acknowledge the help provided by A. L. Vishwakarma and staffs in Sophisticated Analytical Instrumentation Facility (SAIF) in performing flow cytometry experiments. Research work is supported by CSIR-CDRI Network project: "Towards holistic understanding of complex diseases: Unraveling the threads of complex disease (THUNDER) Project No: BSC0102.

Reference

- [1] H.N. Ginsberg, P.R. MacCallum, The obesity, metabolic syndrome, and type 2 diabetes mellitus pandemic: Part I. Increased cardiovascular disease risk and the importance of atherogenic dyslipidemia in persons with the metabolic syndrome and type 2 diabetes mellitus, *Journal of the cardiometabolic syndrome*, 4 (2009) 113-119.
- [2] J.W. Njeru, E.M. Tan, J. St Sauver, D.J. Jacobson, A.A. Agunwamba, P.M. Wilson, L.J. Rutten, S. Damodaran, M.L. Wieland, High Rates of Diabetes Mellitus, Pre-diabetes and Obesity Among Somali Immigrants and Refugees in Minnesota: A Retrospective Chart Review, *Journal of immigrant and minority health*, 18 (2016) 1343-1349.
- [3] F. Ofei, Obesity - a preventable disease, *Ghana medical journal*, 39 (2005) 98-101.
- [4] A.R. Zammit, M.J. Katz, C. Derby, M. Bitzer, R.B. Lipton, Abdominal obesity is a risk factor for dysexecutive function in chronic kidney disease, *Preventive medicine reports*, 4 (2016) 128-133.
- [5] M.H. Pan, Y.C. Tung, G. Yang, S. Li, C.T. Ho, Molecular mechanisms of the anti-obesity effect of bioactive compounds in tea and coffee, *Food & function*, 7 (2016) 4481-4491.
- [6] M. Beg, K. Shankar, S. Varshney, S. Rajan, S.P. Singh, P. Jagdale, A. Puri, B.P. Chaudhari, K.V. Sashidhara, A.N. Gaikwad, A clerodane diterpene inhibit adipogenesis by cell cycle arrest and ameliorate obesity in C57BL/6 mice, *Molecular and cellular endocrinology*, 399 (2015) 373-385.
- [7] Q.A. Wang, C. Tao, R.K. Gupta, P.E. Scherer, Tracking adipogenesis during white adipose tissue development, expansion and regeneration, *Nature medicine*, 19 (2013) 1338-1344.
- [8] A. Soriano-Maldonado, V.A. Aparicio, F.J. Felix-Redondo, D. Fernandez-Berges, Severity of obesity and cardiometabolic risk factors in adults: Sex differences and role of physical activity. The HERMEX study, *International journal of cardiology*, 223 (2016) 352-359.
- [9] Y.H. Han, Z. Li, J.Y. Um, X.Q. Liu, S.H. Hong, Anti-adipogenic effect of Glycoside St-E2 and Glycoside St-C1 isolated from the leaves of *Acanthopanax henryi* (Oliv.) Harms in 3T3-L1 cells, *Bioscience, biotechnology, and biochemistry*, 80 (2016) 2391-2400.
- [10] A. Rabiee, V. Schwammle, S. Sidoli, J. Dai, A. Rogowska-Wrzesinska, S. Mandrup, O.N. Jensen, Nuclear phosphoproteome analysis of 3T3-L1 preadipocyte differentiation reveals system-wide phosphorylation of transcriptional regulators, *Proteomics*, (2016).
- [11] F.J. Ruiz-Ojeda, A.I. Ruperez, C. Gomez-Llorente, A. Gil, C.M. Aguilera, Cell Models and Their Application for Studying Adipogenic Differentiation in Relation to Obesity: A Review, *International journal of molecular sciences*, 17 (2016).

- [12] S. Rajan, A. Gupta, M. Beg, K. Shankar, A. Srivastava, S. Varshney, D. Kumar, A.N. Gaikwad, Adipocyte transdifferentiation and its molecular targets, *Differentiation; research in biological diversity*, 87 (2014) 183-192.
- [13] D. Moseti, A. Regassa, W.K. Kim, Molecular Regulation of Adipogenesis and Potential Anti-Adipogenic Bioactive Molecules, *International journal of molecular sciences*, 17 (2016).
- [14] R. Cereijo, M. Giralt, F. Villarroya, Thermogenic brown and beige/brite adipogenesis in humans, *Annals of medicine*, 47 (2015) 169-177.
- [15] Y. Wang, Y. Mu, H. Li, N. Ding, Q. Wang, S. Wang, N. Wang, Peroxisome proliferator-activated receptor-gamma gene: a key regulator of adipocyte differentiation in chickens, *Poultry science*, 87 (2008) 226-232.
- [16] E.C. Mariman, P. Wang, Adipocyte extracellular matrix composition, dynamics and role in obesity, *Cellular and molecular life sciences : CMLS*, 67 (2010) 1277-1292.
- [17] C. Viegas-Junior, A. Danuello, V. da Silva Bolzani, E.J. Barreiro, C.A. Fraga, Molecular hybridization: a useful tool in the design of new drug prototypes, *Current medicinal chemistry*, 14 (2007) 1829-1852.
- [18] V.S. Velezheva, P.J. Brennan, V.Y. Marshakov, D.V. Gusev, I.N. Lisichkina, A.S. Peregudov, L.N. Tchernousova, T.G. Smirnova, S.N. Andreevskaya, A.E. Medvedev, Novel pyridazino[4,3-b]indoles with dual inhibitory activity against *Mycobacterium tuberculosis* and monoamine oxidase, *Journal of medicinal chemistry*, 47 (2004) 3455-3461.
- [19] A. Andreani, S. Burnelli, M. Granaiola, A. Leoni, A. Locatelli, R. Morigi, M. Rambaldi, L. Varoli, L. Landi, C. Prata, M.V. Berridge, C. Grasso, H.H. Fiebig, G. Kelter, A.M. Burger, M.W. Kunkel, Antitumor activity of bis-indole derivatives, *Journal of medicinal chemistry*, 51 (2008) 4563-4570.
- [20] K.E. Knott, S. Auschill, A. Jager, H.J. Knolker, First total synthesis of the whole series of the antiostatins A and B, *Chem Commun (Camb)*, (2009) 1467-1469.
- [21] G.L. Regina, A. Coluccia, F. Piscitelli, A. Bergamini, A. Sinistro, A. Cavazza, G. Maga, A. Samuele, S. Zanolli, E. Novellino, M. Artico, R. Silvestri, Indolyl aryl sulfones as HIV-1 non-nucleoside reverse transcriptase inhibitors: role of two halogen atoms at the indole ring in developing new analogues with improved antiviral activity, *Journal of medicinal chemistry*, 50 (2007) 5034-5038.
- [22] P.D. Pierson, A. Fettes, C. Freichel, S. Gatti-McArthur, C. Hertel, J. Huwyler, P. Mohr, T. Nakagawa, M. Nettekoven, J.M. Plancher, S. Raab, H. Richter, O. Roche, R.M. Rodriguez Sarmiento, M. Schmitt, F. Schuler, T. Takahashi, S. Taylor, C. Ullmer, R. Wiegand, 5-hydroxyindole-2-carboxylic acid amides: novel histamine-3 receptor inverse agonists for the treatment of obesity, *Journal of medicinal chemistry*, 52 (2009) 3855-3868.
- [23] K.V. Sashidhara, A. Kumar, M. Kumar, A. Srivastava, A. Puri, Synthesis and antihyperlipidemic activity of novel coumarin bisindole derivatives, *Bioorganic & medicinal chemistry letters*, 20 (2010) 6504-6507.
- [24] F. Lehmann, S. Haile, E. Axen, C. Medina, J. Uppenberg, S. Svensson, T. Lundback, L. Rondahl, T. Barf, Discovery of inhibitors of human adipocyte fatty acid-binding protein, a potential type 2 diabetes target, *Bioorganic & medicinal chemistry letters*, 14 (2004) 4445-4448.
- [25] S.J. Yan, Y.J. Liu, Y.L. Chen, L. Liu, J. Lin, An efficient one-pot synthesis of heterocycle-fused 1,2,3-triazole derivatives as anti-cancer agents, *Bioorganic & medicinal chemistry letters*, 20 (2010) 5225-5228.
- [26] X.L. Wang, K. Wan, C.H. Zhou, Synthesis of novel sulfanilamide-derived 1,2,3-triazoles and their evaluation for antibacterial and antifungal activities, *European journal of medicinal chemistry*, 45 (2010) 4631-4639.
- [27] P. Shanmugavelan, S. Nagarajan, M. Sathishkumar, A. Ponnuswamy, P. Yogeewari, D. Sriram, Efficient synthesis and in vitro antitubercular activity of 1,2,3-triazoles as inhibitors of *Mycobacterium tuberculosis*, *Bioorganic & medicinal chemistry letters*, 21 (2011) 7273-7276.

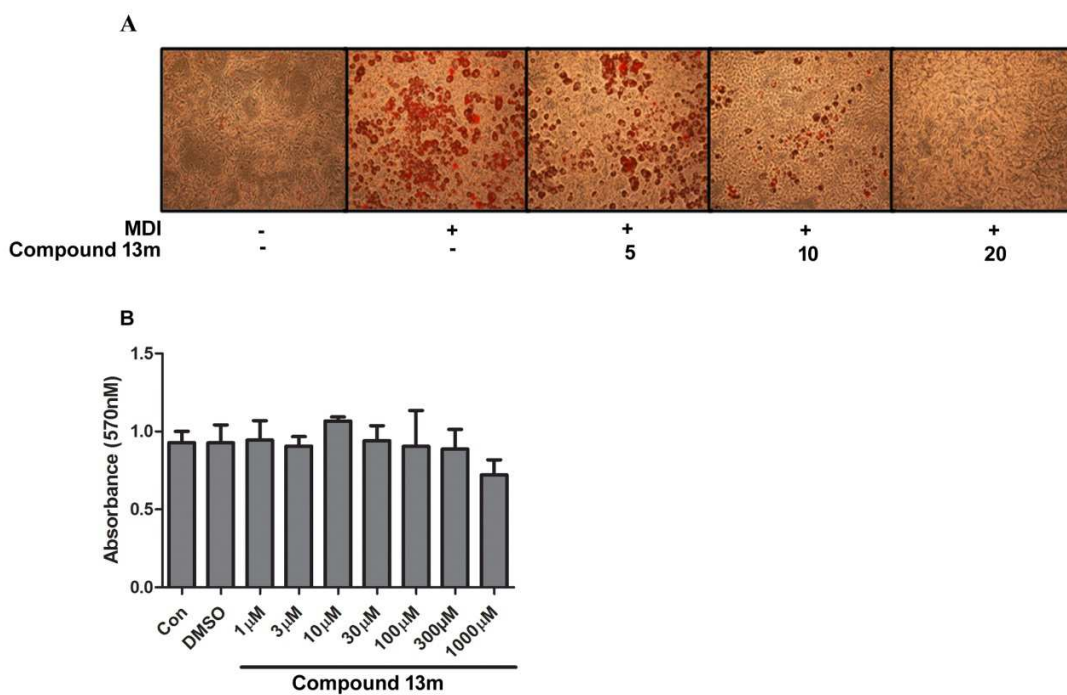
- [28] H. Behbehani, H.M. Ibrahim, S. Makhseed, H. Mahmoud, Applications of 2-arylhydrazononitriles in synthesis: preparation of new indole containing 1,2,3-triazole, pyrazole and pyrazolo[1,5-a]pyrimidine derivatives and evaluation of their antimicrobial activities, *European journal of medicinal chemistry*, 46 (2011) 1813-1820.
- [29] A.K. Jordao, P.P. Afonso, V.F. Ferreira, M.C. de Souza, M.C. Almeida, C.O. Beltrame, D.P. Paiva, S.M. Wardell, J.L. Wardell, E.R. Tiekink, C.R. Damaso, A.C. Cunha, Antiviral evaluation of N-amino-1,2,3-triazoles against Cantagalo virus replication in cell culture, *European journal of medicinal chemistry*, 44 (2009) 3777-3783.
- [30] C. da Silva Fde, M.C. de Souza, Frugulhetti, II, H.C. Castro, S.L. Souza, T.M. de Souza, D.Q. Rodrigues, A.M. Souza, P.A. Abreu, F. Passamani, C.R. Rodrigues, V.F. Ferreira, Synthesis, HIV-RT inhibitory activity and SAR of 1-benzyl-1H-1,2,3-triazole derivatives of carbohydrates, *European journal of medicinal chemistry*, 44 (2009) 373-383.
- [31] S. Shafi, M.M. Alam, N. Mulakayala, C. Mulakayala, G. Vanaja, A.M. Kalle, R. Pallu, M.S. Alam, Synthesis of novel 2-mercapto benzothiazole and 1,2,3-triazole based bis-heterocycles: their anti-inflammatory and anti-nociceptive activities, *European journal of medicinal chemistry*, 49 (2012) 324-333.
- [32] A.K. Jordao, V.F. Ferreira, T.M. Souza, G.G. Faria, V. Machado, J.L. Abrantes, M.C. de Souza, A.C. Cunha, Synthesis and anti-HSV-1 activity of new 1,2,3-triazole derivatives, *Bioorganic & medicinal chemistry*, 19 (2011) 1860-1865.
- [33] J.L. Kelley, C.S. Koble, R.G. Davis, E.W. McLean, F.E. Soroko, B.R. Cooper, 1-(Fluorobenzyl)-4-amino-1H-1,2,3-triazolo[4,5-c]pyridines: synthesis and anticonvulsant activity, *Journal of medicinal chemistry*, 38 (1995) 4131-4134.
- [34] H.H. Kinfe, Y.H. Belay, J.S. Joseph, E. Mukwevho, Evaluation of the Influence of thiosemicarbazone-triazole hybrids on genes implicated in lipid oxidation and accumulation as potential anti-obesity agents, *Bioorganic & medicinal chemistry letters*, 23 (2013) 5275-5278.
- [35] P. Kothandaraman, S.R. Mothe, S.S. Toh, P.W. Chan, Gold-catalyzed cycloisomerizations of 1-(2-(tosylamino)phenyl)prop-2-yn-1-ols to 1H-indole-2-carbaldehydes and (E)-2-(iodomethylene)indolin-3-ols, *The Journal of organic chemistry*, 76 (2011) 7633-7640.
- [36] H. Hochegger, S. Takeda, T. Hunt, Cyclin-dependent kinases and cell-cycle transitions: does one fit all?, *Nature reviews. Molecular cell biology*, 9 (2008) 910-916.
- [37] J. Liu, H. Wang, Y. Zuo, S.R. Farmer, Functional interaction between peroxisome proliferator-activated receptor gamma and beta-catenin, *Molecular and cellular biology*, 26 (2006) 5827-5837.
- [38] H. Waki, K.W. Park, N. Mitro, L. Pei, R. Damoiseaux, D.C. Wilpitz, K. Reue, E. Saez, P. Tontonoz, The small molecule harmine is an antidiabetic cell-type-specific regulator of PPARgamma expression, *Cell metabolism*, 5 (2007) 357-370.
- [39] R. Gedaly, R. Galuppo, M.F. Daily, M. Shah, E. Maynard, C. Chen, X. Zhang, K.A. Esser, D.A. Cohen, B.M. Evers, J. Jiang, B.T. Spear, Targeting the Wnt/beta-catenin signaling pathway in liver cancer stem cells and hepatocellular carcinoma cell lines with FH535, *PloS one*, 9 (2014) e99272.
- [40] W. Kong, J. Wei, P. Abidi, M. Lin, S. Inaba, C. Li, Y. Wang, Z. Wang, S. Si, H. Pan, S. Wang, J. Wu, Z. Li, J. Liu, J.D. Jiang, Berberine is a novel cholesterol-lowering drug working through a unique mechanism distinct from statins, *Nature medicine*, 10 (2004) 1344-1351.
- [41] C.Y. Kim, T.T. Le, C. Chen, J.X. Cheng, K.H. Kim, Curcumin inhibits adipocyte differentiation through modulation of mitotic clonal expansion, *The Journal of nutritional biochemistry*, 22 (2011) 910-920.
- [42] S. Varshney, K. Shankar, M. Beg, V.M. Balamnavar, S.K. Mishra, P. Jagdale, S. Srivastava, Y.S. Chhonker, V. Lakshmi, B.P. Chaudhari, R.S. Bhatta, A.K. Saxena, A.N. Gaikwad, Rohitukine inhibits in vitro adipogenesis arresting mitotic clonal expansion and improves dyslipidemia in vivo, *Journal of lipid research*, 55 (2014) 1019-1032.

- [43] K. Shankar, S.K. Singh, D. Kumar, S. Varshney, A. Gupta, S. Rajan, A. Srivastava, M. Beg, A.K. Srivastava, S. Kanojiya, D.K. Mishra, A.N. Gaikwad, Cucumis melo ssp. Agrestis var. Agrestis Ameliorates High Fat Diet Induced Dyslipidemia in Syrian Golden Hamsters and Inhibits Adipogenesis in 3T3-L1 Adipocytes, *Pharmacognosy magazine*, 11 (2015) S501-510.
- [44] Z. Zhang, H. Wang, R. Jiao, C. Peng, Y.M. Wong, V.S. Yeung, Y. Huang, Z.Y. Chen, Choosing hamsters but not rats as a model for studying plasma cholesterol-lowering activity of functional foods, *Molecular nutrition & food research*, 53 (2009) 921-930.
- [45] M. Treguier, F. Briand, A. Boubacar, A. Andre, T. Magot, P. Nguyen, M. Krempf, T. Sulpice, K. Ouguerram, Diet-induced dyslipidemia impairs reverse cholesterol transport in hamsters, *European journal of clinical investigation*, 41 (2011) 921-928.
- [46] K. Nakaya, J. Tohyama, S.U. Naik, H. Tanigawa, C. MacPhee, J.T. Billheimer, D.J. Rader, Peroxisome proliferator-activated receptor- α activation promotes macrophage reverse cholesterol transport through a liver X receptor-dependent pathway, *Arteriosclerosis, thrombosis, and vascular biology*, 31 (2011) 1276-1282.
- [47] J. Frith, P. Genever, Transcriptional control of mesenchymal stem cell differentiation, *Transfusion medicine and hemotherapy : offizielles Organ der Deutschen Gesellschaft fur Transfusionsmedizin und Immunhamatologie*, 35 (2008) 216-227.
- [48] Y. Hu, G.E. Davies, Berberine increases expression of GATA-2 and GATA-3 during inhibition of adipocyte differentiation, *Phytomedicine : international journal of phytotherapy and phytopharmacology*, 16 (2009) 864-873.
- [49] T. Horikawa, T. Shimada, Y. Okabe, K. Kinoshita, K. Koyama, K. Miyamoto, K. Ichinose, K. Takahashi, M. Aburada, Polymethoxyflavonoids from *Kaempferia parviflora* induce adipogenesis on 3T3-L1 preadipocytes by regulating transcription factors at an early stage of differentiation, *Biological & pharmaceutical bulletin*, 35 (2012) 686-692.
- [50] K.M. Choi, Y.S. Lee, D.M. Sin, S. Lee, M.K. Lee, Y.M. Lee, J.T. Hong, Y.P. Yun, H.S. Yoo, Sulforaphane inhibits mitotic clonal expansion during adipogenesis through cell cycle arrest, *Obesity (Silver Spring)*, 20 (2012) 1365-1371.
- [51] H. Kim, K. Sakamoto, (-)-Epigallocatechin gallate suppresses adipocyte differentiation through the MEK/ERK and PI3K/Akt pathways, *Cell biology international*, 36 (2012) 147-153.
- [52] M.C. Mitterberger, W. Zwerschke, Mechanisms of resveratrol-induced inhibition of clonal expansion and terminal adipogenic differentiation in 3T3-L1 preadipocytes, *The journals of gerontology. Series A, Biological sciences and medical sciences*, 68 (2013) 1356-1376.
- [53] J.Y. Kwon, S.G. Seo, S. Yue, J.X. Cheng, K.W. Lee, K.H. Kim, An inhibitory effect of resveratrol in the mitotic clonal expansion and insulin signaling pathway in the early phase of adipogenesis, *Nutr Res*, 32 (2012) 607-616.
- [54] H.J. Chen, L.S. Hsu, Y.T. Shia, M.W. Lin, C.M. Lin, The beta-catenin/TCF complex as a novel target of resveratrol in the Wnt/beta-catenin signaling pathway, *Biochemical pharmacology*, 84 (2012) 1143-1153.
- [55] C.N. Bennett, S.E. Ross, K.A. Longo, L. Bajnok, N. Hemati, K.W. Johnson, S.D. Harrison, O.A. MacDougald, Regulation of Wnt signaling during adipogenesis, *The Journal of biological chemistry*, 277 (2002) 30998-31004.
- [56] H.J. Yun, J.H. Kim, H.Y. Jeong, H.H. Ji, S.W. Nam, E.W. Lee, B.W. Kim, H.J. Kwon, Widdrol blocks 3T3-L1 preadipocytes growth and differentiation due to inhibition of mitotic clonal expansion, *Journal of microbiology and biotechnology*, 22 (2012) 806-813.
- [57] M. Laudes, Role of WNT signalling in the determination of human mesenchymal stem cells into preadipocytes, *Journal of molecular endocrinology*, 46 (2011) R65-72.

- [58] A. Bowen, K. Kos, J. Whatmore, S. Richardson, H.J. Welters, Wnt4 antagonises Wnt3a mediated increases in growth and glucose stimulated insulin secretion in the pancreatic beta-cell line, INS-1, *Biochemical and biophysical research communications*, 479 (2016) 793-799.
- [59] M. Kim, S. Kim, S.H. Lee, W. Kim, M.J. Sohn, H.S. Kim, J. Kim, E.H. Jho, Merlin inhibits Wnt/beta-catenin signaling by blocking LRP6 phosphorylation, *Cell death and differentiation*, 23 (2016) 1638-1647.
- [60] D. Ouyang, L. Xu, L. Zhang, D. Guo, X. Tan, X. Yu, J. Qi, Y. Ye, Q. Liu, Y. Ma, Y. Li, MiR-181a-5p regulates 3T3-L1 cell adipogenesis by targeting Smad7 and Tcf7l2, *Acta biochimica et biophysica Sinica*, 48 (2016) 1034-1041.
- [61] Y. Lecarpentier, A. Vallee, Opposite Interplay between PPAR Gamma and Canonical Wnt/Beta-Catenin Pathway in Amyotrophic Lateral Sclerosis, *Frontiers in neurology*, 7 (2016) 100.
- [62] Y.S. Chen, R. Wu, X. Yang, S. Kou, O.A. MacDougald, L. Yu, H. Shi, B. Xue, Inhibiting DNA methylation switches adipogenesis to osteoblastogenesis by activating Wnt10a, *Scientific reports*, 6 (2016) 25283.
- [63] D.W. Garnick, K. Swartz, K.C. Skwara, Insurance agents: ignored players in health insurance reform, *Health Aff (Millwood)*, 17 (1998) 137-143.
- [64] B. Staels, J. Dallongeville, J. Auwerx, K. Schoonjans, E. Leitersdorf, J.C. Fruchart, Mechanism of action of fibrates on lipid and lipoprotein metabolism, *Circulation*, 98 (1998) 2088-2093.
- [65] M. Pawlak, P. Lefebvre, B. Staels, Molecular mechanism of PPARalpha action and its impact on lipid metabolism, inflammation and fibrosis in non-alcoholic fatty liver disease, *Journal of hepatology*, 62 (2015) 720-733.
- [66] B. Staels, M. Maes, A. Zambon, Fibrates and future PPARalpha agonists in the treatment of cardiovascular disease, *Nature clinical practice. Cardiovascular medicine*, 5 (2008) 542-553.

Supplementary Figure 1

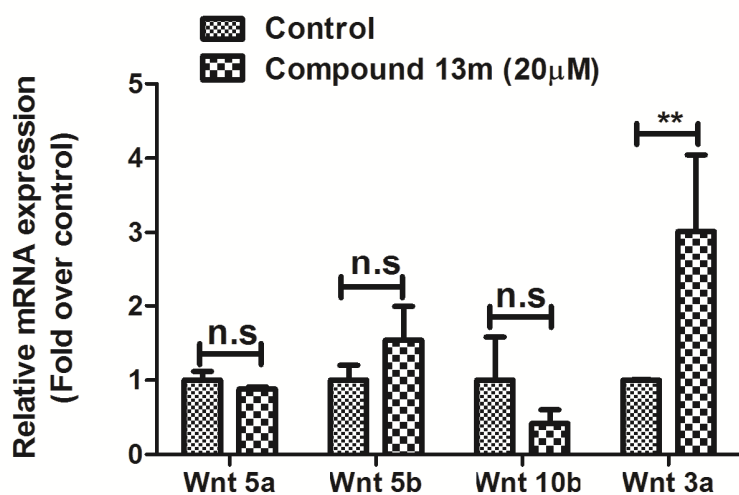
Oil red O staining images of 3T3L1 differentiated adipocytes treated with $5\mu\text{M}$, $10\mu\text{M}$ and $20\mu\text{M}$ of compound **13m** along with differentiation media. Images were capture at 10x magnification with Leica microscope (A). 3T3L1 adipocytes were treated with varying concentration of compound **13m** and MTT assay was performed. Absorbance was taken at 570 nM. n=3, error bars represent SD (B).

Supplementary Figure 1

Supplementary Figure: 2

Quantitative gene expression analysis of wnt5A, wnt5B, wnt10a and wnt3a in 3T3L1 cells treated with MDI in presence and absence of compound **13m** ($20\mu\text{M}$). $n=3$, errorbars represent mean \pm SD. $**P<0.01$ as tested by one way ANOVA followed by Bonferroni posttest analysis.

A)

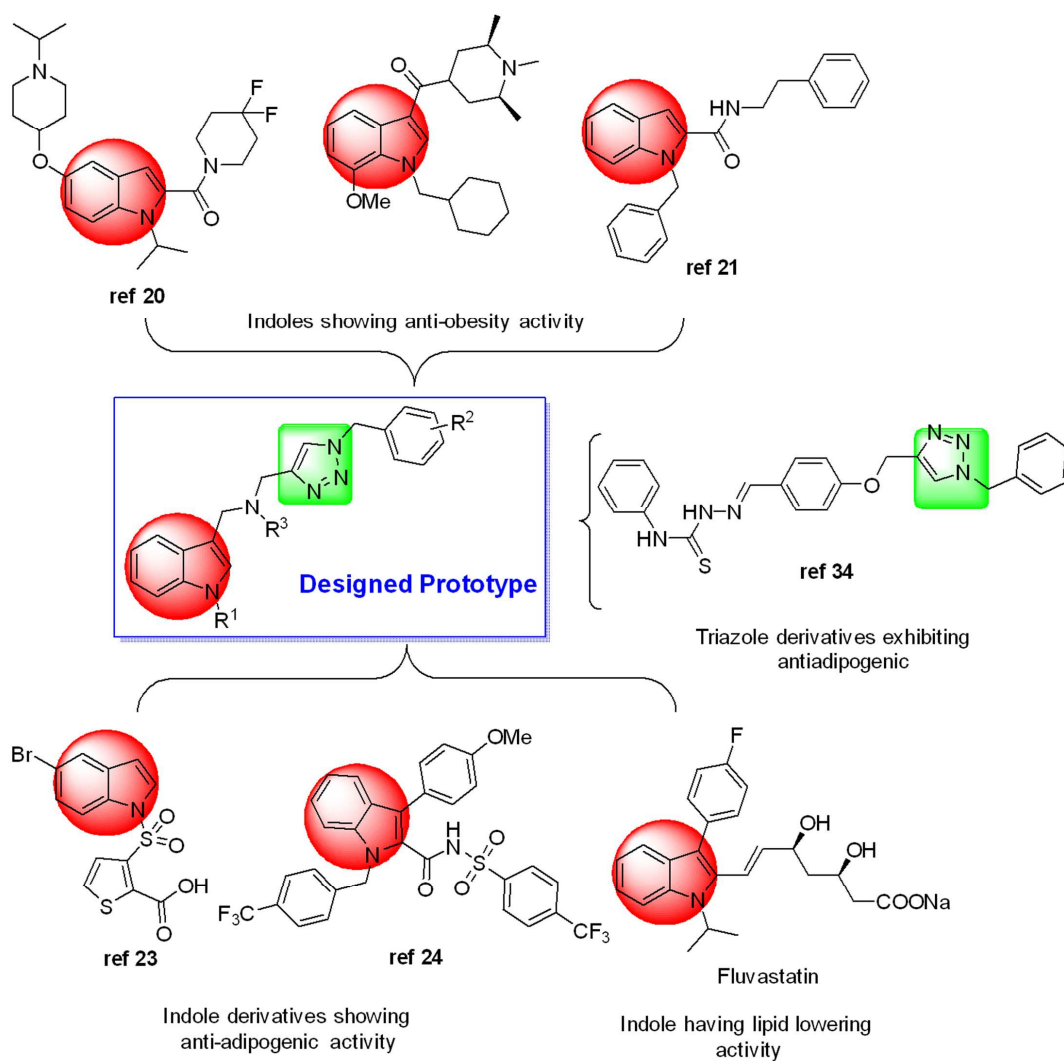


Supplementary table 1: *In Vitro* Anti-Adipogenic Activity Of Triazole/Indole Hybrid

Derivatives

Compound (20 μ M)	adipogenesis inhibition (%)	Significance (p value)	Standard Deviation
8a	0.03	n.s (0.99)	10.5
8b	-7.6	n.s (0.57)	22.3
8c	-10.9	n.s (0.34)	19.1
8d	-5.9	n.s (0.47)	14.3
8e	-22	n.s (0.07)	16.3
8f	-20.8	n.s (0.16)	22.3
13a	3.4	n.s (0.51)	9
13b	-18	n.s (0.15)	13.9
13c	1	n.s (0.90)	16.5
13d	7.6	n.s (0.26)	11
13e	-18	n.s (0.15)	13.9
13f	-22	* (0.032)	7
13g	-4.8	n.s (0.35)	8.7
13h	-21	n.s (0.09)	7
13i	-19.5	n.s (0.05)	8.2
13j	12.3	n.s (0.06)	8.4
13k	-6.5	n.s (0.38)	10.1
13l	3.4	n.s (0.44)	6.2
13m	71.5	*** (0.0001)	0.8
13n	39.5	*** (0.0001)	0.6
13o	31.9	*** (0.0008)	1.5
18a	46	*** (0.0003)	4.6
18b	-13.9	** (0.007)	4.3
18c	57.5	*** (0.0001)	1.6
18d	-3.3	n.s (0.2)	4.1
18e	-5.5	n.s (0.2)	6.9
18f	-13.1	** (0.004)	3.5
18g	21	*** (0.0003)	2.2
18h	-35	*** (0.0002)	3.3
18i	25.8	*** (0.0005)	3.2
18j	-52.3	*** (0.0001)	2.6
18k	-20	** (0.004)	5.2
18l	-1.7	n.s (0.28)	2.6
21a	-38.5	*** (0.0002)	3.3
21b	-35.7	** (0.0045)	9.2
21c	-81.9	*** (0.0001)	3.7
21d	-97.7	*** (0.0001)	2
21e	-53.4	*** (0.0001)	3.2
21f	-39.8	*** (0.0001)	1.3

The negative inhibition values indicate pro-adipogenic activity of the compounds (Red). The positive inhibition values indicate anti-adipogenic activity of the compounds (Green) as depicted in table. Student *t* test was used to calculate significance between control and compound treated group. (n.s represent Non Significant, * represents P value <0.05, ** represent P value <0.01, *** represent P. value<0.001).



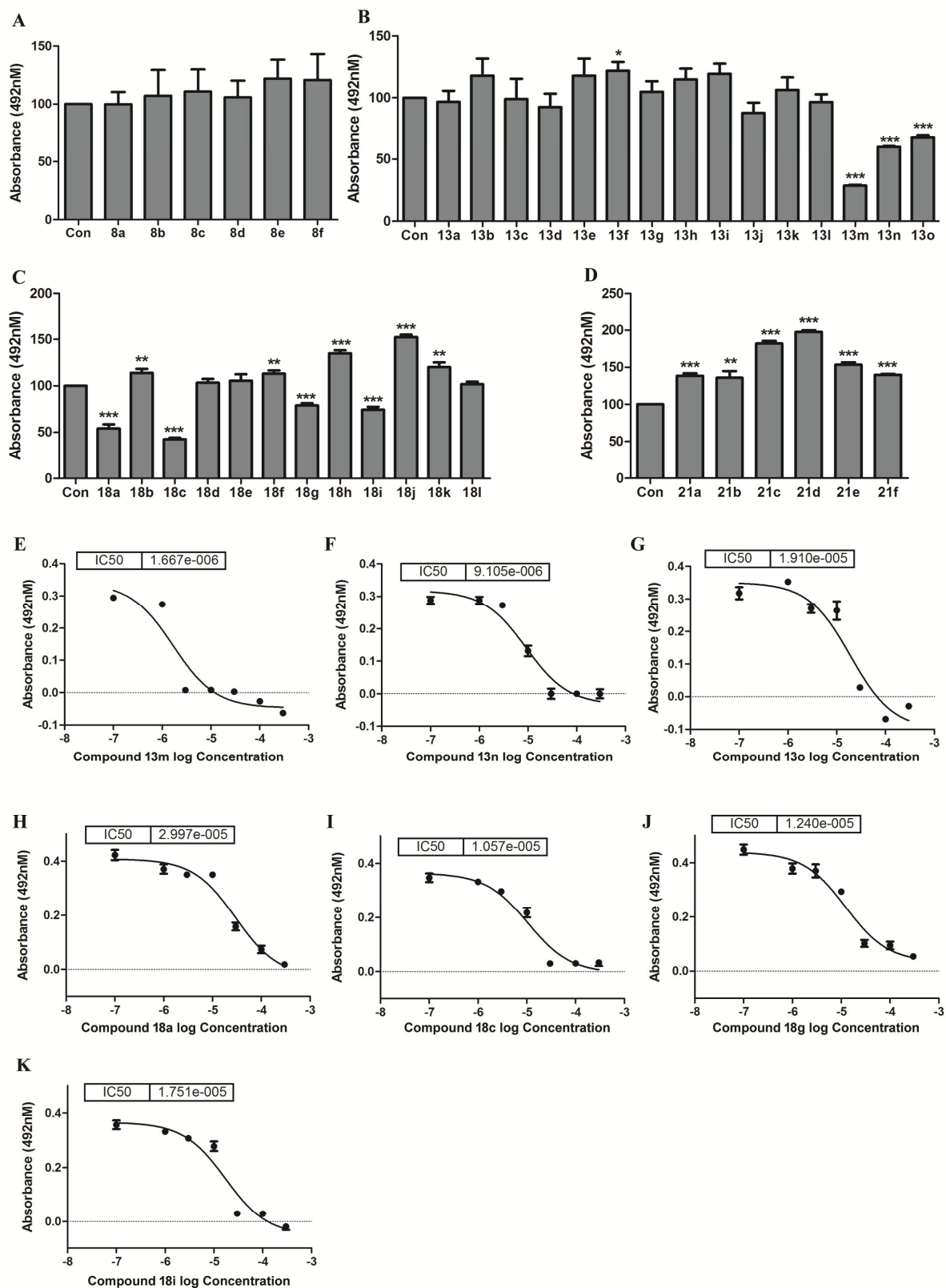


Figure 1

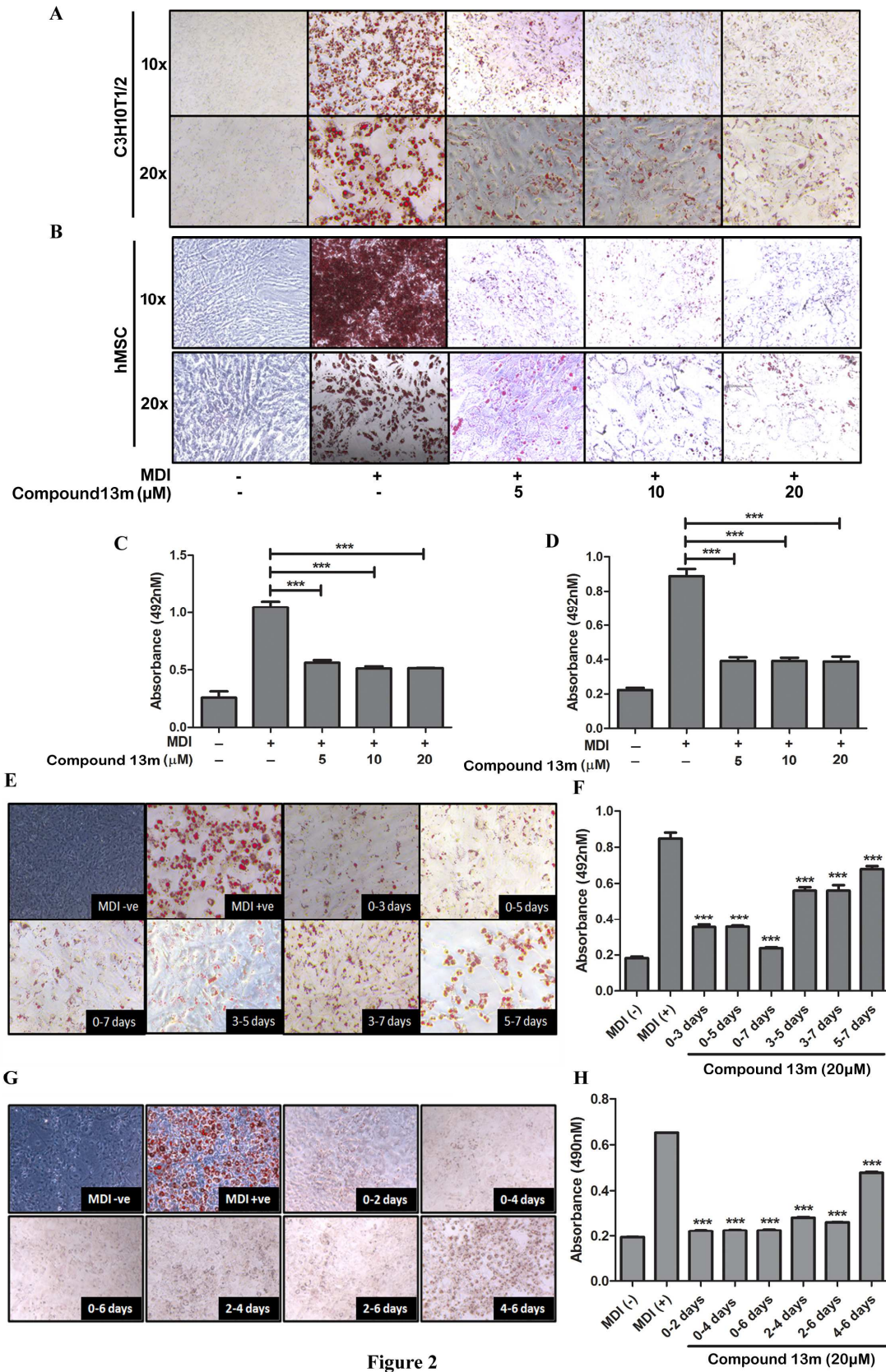


Figure 2

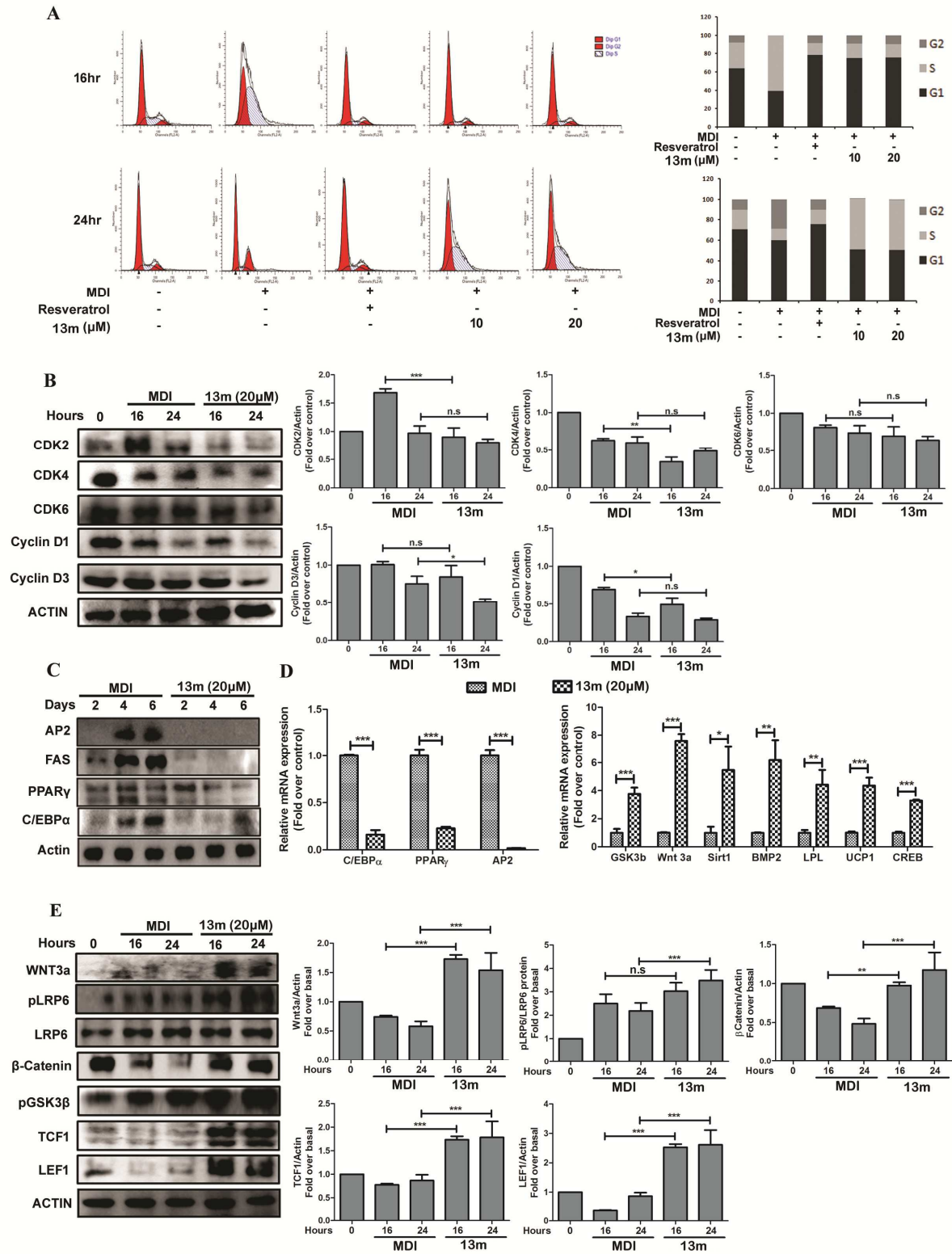
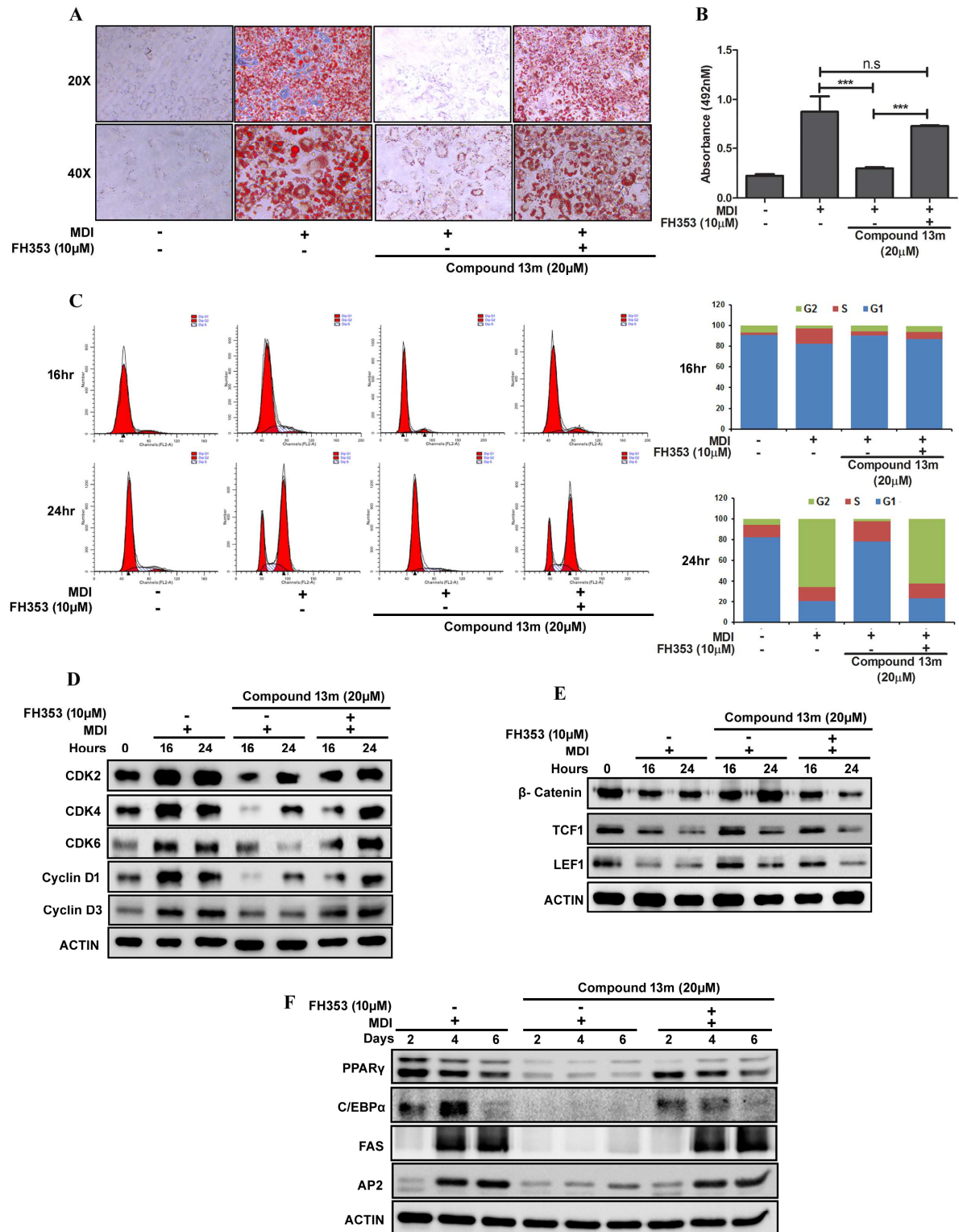


Figure- 3



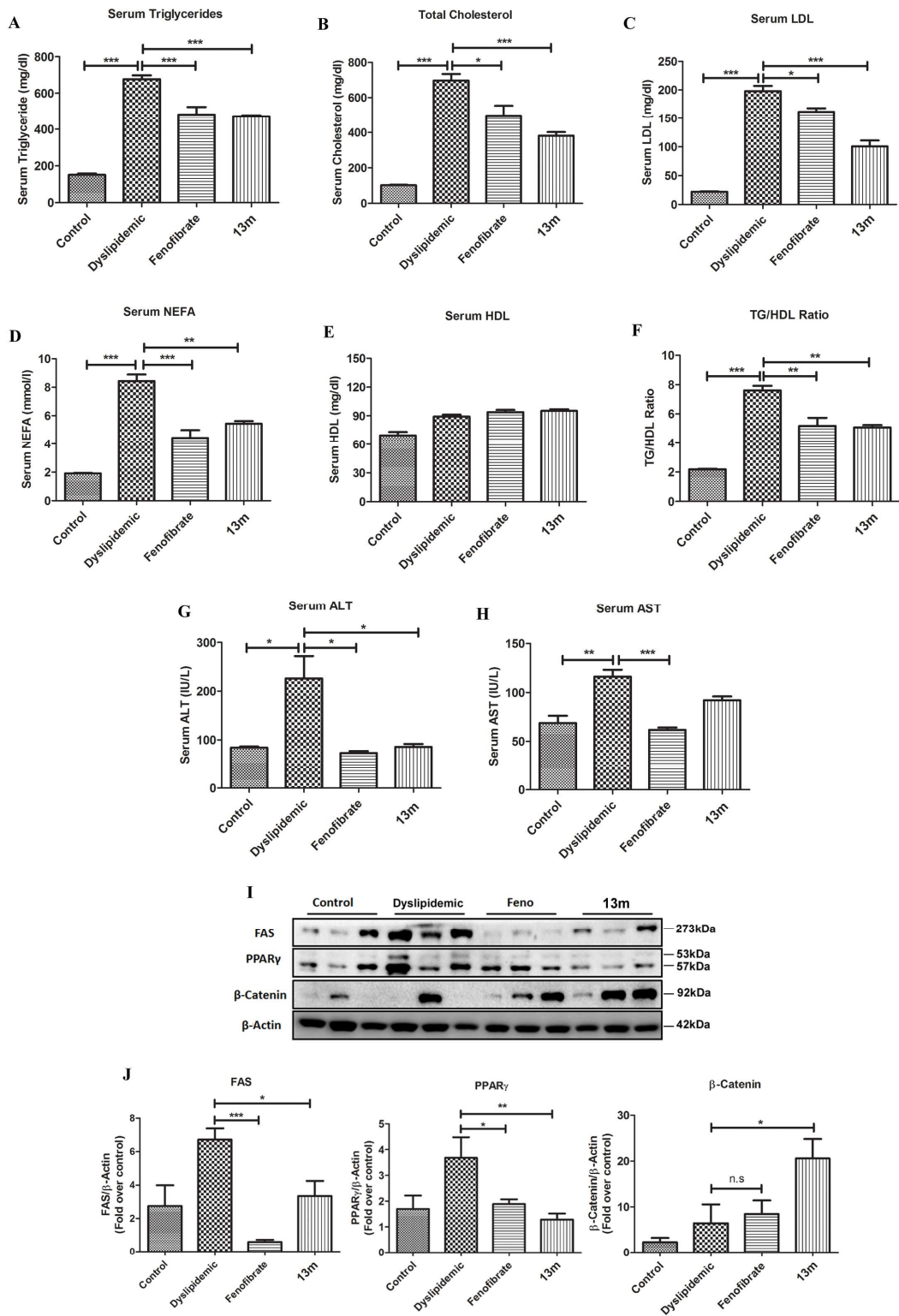
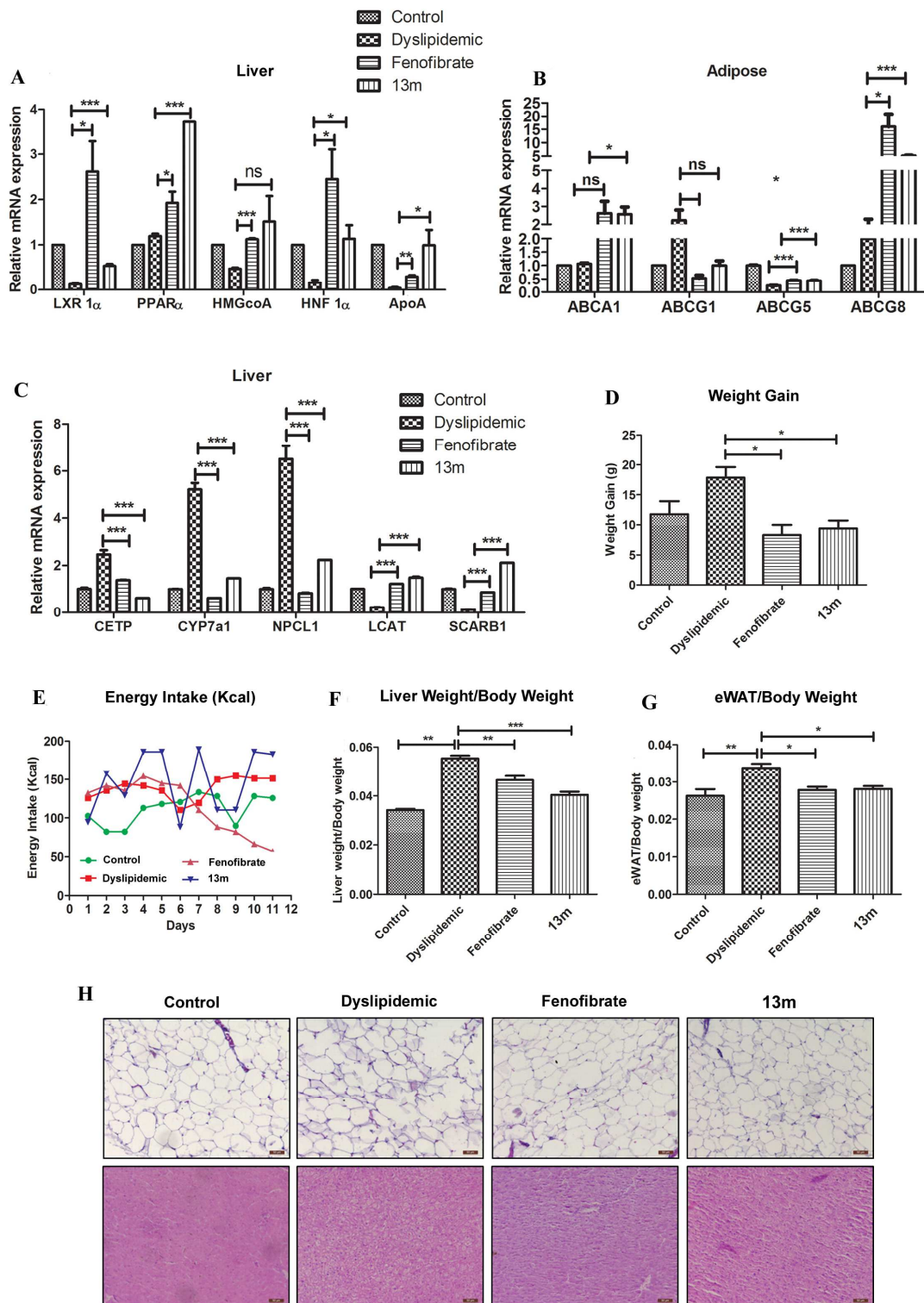


Figure 5



Highlights

- Compound **13m** a hybrid derivative of indole and triazole shows potent anti-adipogenic activity with the IC-50 value of 1.67 μ M.
- Compound **13m** arrest cell cycle at G1/S phase by activating wnt3a/ β catenin pathway.
- Compound **13m** improves dyslipidemia by activating reverse cholesterol transport in HFD fed Syrian golden hamster.
- Overall this study provides a unique perspective into the anti-adipogenic/antidyslipidemic property of triazole and indole hybrids.